Ministère de l'Enseignement Supérieur
et de la Recherche Scientifique
Université de Carthage
École Polytechnique de Tunisie

وزارة التعليم العالي و البحث العلمي
جامعة قرطاج
المدرسة التونسية للتقنيات

# Brain tissues classification on MRI Scans using a Robust and Evidential Fuzzy C-means Algorithm

**by :**

**MS. Arij BEN TEJ**

Presented to the **Tunisia Polytechnic School**

in partial fulfillment of the requirements for the degree of

MASTER OF SCIENCE

in

**Advanced Engineering - Complex and Intelligent Systems**

Defended on 16 December 2021, in front of the examination committee:

| | |
|---|---|
| Prof. Lilia El AMRAOUI : | **President** |
| Dr. Haythem GHAZOUANI : | **Reviewer** |
| Prof. Khaled NOURI : | **Supervisor (LSA-EPT)** |
| Dr. Khaoula BEDOUI : | **Supervisor (LIMTIC)** |

**Master Thesis Prepared at**

Laboratory of Advanced Systems

& Computer Science, Modeling and Information and Knowledge Processing research Laboratory

LIMTIC

Academic year

2020-2021

# *Dedication*

Every work needs self-efforts as well as guidance from others, especially those who were very close to the heart.

I dedicate these lines to express from the bottom of my heart my gratitude towards all the people who helped me to complete this master thesis.

At first, I would like to express my love and affection to my dear parents Amel HANAFI and Yassin BENTEJ for all the sacrifices they made for me to be here.

I would like to thank my sisters Ichrak BENTEJ, Siwar ABBES and Linda BEZINE for believing in me and for their presence by my side.

I also want to thank my friend and tutor, Amal JLASSI for her support and encouragement.

*Arij.*

# *Acknowlegments*

*"Keep away from people who try to belittle your ambitions. Small people always do that, but, the really great make you feel that too, can become great."*

*Mark Twain*

It is a great pleasure for me in acknowledging my deep sense of gratitude to all those who have helped me in completing this project successfully.

I would like to thank **Mrs. Khaoula BEDOUI** and **Mr. Khaled NOURI**, my supervisors, for giving me the chance to work on this subject and for their guidance which allowed me to progress in the accomplishment of this thesis. I also choose this moment to acknowledge the contribution of **Mrs. Amal JLASSI**, my master thesis tutor, gratefully, she is always offering help and giving prompt replies to my questions.

I also extend my sense of gratitude to all who, directly and indirectly, have provided me with any kind of help during this project.

Finally, I wish to express the honour for having the jury members agree to give us their attention and evaluate our work.

# Contents

# List of Figures

# List of Tables

# List of Equations

# Acronyms

**CNS**: Central Nervous System.

**AD**: Alzheimer's disease.

**WHO**: World Health Organization.

**MRI**: Magnetic Resonance Imaging.

**PET**: Positron Emission Tomography.

**NMR**: Nuclear Magnetic Resonance.

**RF**: Radio Frequency.

**WM**: White Matter.

**CSF**: Cerebrospinal Fluid.

**TR**:Repetition Time.

**TE**: Time to Echo.

**FLAIR**:Fluid Attenuated Inversion Recovery.

**PD**:Proton Density.

**SNR**: Signal to Noise Ratio.

**GM**:Gray Matter.

**BMS**: Brain MRI Segmentation.

**FCM**: Fuzzy C-Means.

**SVM**: Support Vector Machine.

**MRF**:Markov Random Fields.

**EnFCM**: Enhanced Fuzzy C-Means.

**FGFCM**:Fast Generalized Fuzzy C-Means.

**FLICM**: Fuzzy Local Information C-Means.

**KWFLICM**: kernel weighted fuzzy local information c-mean

**NWFCM**: neighborhood weighted FCM

**FRFCM**: Fast and robust FCM

**DST**: Dempster Shafer Theory

**DT**: Decision Tree

**CART**: Classification And Regression Trees.

**REFCM**: Robust and Evidential FCM

**MV**: Membership values

**NU**: No uncertainty

**SU**: Semi uncertainty

**PU**: Perfect Uncertainty.

**PUSU**: both perfect uncertainty and semi uncertainty

**GT**: Ground Truth

**TP**:True Positive.

**TN**: True Negative.

**FP**:False Positive

**FN**: False Negative

**DC**: Dice Coefficient

**IN**: Intensity Non-uniformity

# General Introduction

In recent years, Magnetic Resonance Imaging (MRI) has become the most commonly used imaging technology in brain medicine and cognitive neuroscience. In fact, it provides a detailed observation of the cerebral tissues and the brain structures as well as the possibility to visualize the brain activity and explore the connectivity of the brain areas.Thus, it represents an essential tool for the diagnosis and the detection of several neurological disorders.

In this context, MRI images segmentation presents the key process in image analysis and interpretation that helps to make better results. However, the traditional approach of manual segmentation is time consuming and needs a high level of accuracy which cannot always be achieved leading even to misdiagnosis. As a result, this process need to be automated using segmentation algorithms that can separate the brain into different regions based on the application interest. However, due to the presence of several artifacts such as noise that can affect the image quality, brain MRI segmentation is challenging.

"A world with an increasing number of questions needs people who contribute solutions". That is why, over the past two decades, brain MRI segmentation has been an active area of research. Thus, several algorithms and contributions were proposed to overcome the challenges and to produce better results. But the results still can be improved with the help of research and technology in the favor of humanity.

Our master thesis subject is related to this context and consists in developing a new Machine Learning method for the classification and segmentation of three brain tissues from MRI images. This report summarizes our work and it is structured as follows:

- The first chapter focuses on medical imaging, its artifacts and its challenges. We present the clinical motivation and the different medical imaging techniques and MRI in particular.

- The second chapter explains the different approaches of MRI image segmentation and classification, presents the different methods proposed in literature and introduces the concept of data fusion.
- The third chapter explains in details our proposed method for brain tissues segmentation and classification from MRI images. Then, this method is evaluated with different evaluation metrics as well as it is compared to different state-of-the-art methods.

Finally, we summarize the main contributions of our conducted work and we open some future works that can enrich it.

# Chapter 1

# Contextualisation

## 1.1 Introduction

In this chapter, we will describe the general context of our research. Firstly, we will review the importance of brain tissues in several diseases' prediction. Then, we will present the different techniques of medical imaging and their evolution over time. Last but not least, we will explore some details about the magnetic resonance imaging. Finally, we will focus on the challenges of our research work as well as its objectives.

## 1.2 Clinical motivation

The specialty of humankind resides in the nervous system, more than any other organ. The human central nervous system (CNS) is the most complex and elegant computing machine that has ever existed [1]. It processes and interprets sensory information and controls a variety of complex motor behaviors. Given the nervous system's intricacy, one would wonder if it can ever be completely comprehended. Indeed, the neuroscientific knowledge has begun to provide a precise and a detailed description of the nervous system's structure and the alterations in its function that occur in different diseases [1].

The nervous system can be damaged by several disorders such as infections, structural disorders and degeneration. Nowadays, the degenerative diseases are becoming more and more common. In fact, neurodegenerative diseases represent a large group of neurological disorders with heterogeneous clinical and pathological expressions affecting specific subsets of neurons in specific functional anatomic systems [2]. This type of disorders includes Alzheimer's disease (AD) that causes memory loss and destroys thinking and problem-solving skills. Besides, it becomes worse through the time. The beginning of AD is 20 years before symptoms arise in which several changes happen to the brain and the affected person cannot notice them [3]. That is why, an effective diagnosis is always in the favor of the patient to be treated better by their doctors.

Another rising illness that can affect the nervous system is the COVID-19 that is a pandemic spreading all over the world since 2019. More than 249 million people had the COVID-19 until now according to the World Health Organization (WHO) [4]. The symptoms of this disease are basically in the respiratory system of the affected person. However, growing evidence indicates that COVID-19 not only attacks the lungs and heart, but also affects the CNS [5]. Many brain tissues went through changes especially for the patients having severe diseases. Given the newness of this illness, previous studies focused on the immediate effect of COVID-19 and left the long-term impact unknown [5]. From that point, several studies and diagnosis must be performed to insure a good treatment for the patients in the future.

As we have previously seen, some brain changes can be unnoticeable for the affected person and an early diagnosis of the brain anomaly leads to an effective treatment and a high healing rate. Thus, many powerful medical imaging analysis tools can be used for this purpose. These artificial vision tools can provide important quantitative information to experts.

Based on the clinician expertise and these medical imaging analysis tools, a diagnosis will be assigned to the patient. However, the quality of these tools depends on the used medical images and the employed techniques. Therefore, it is highly important to understand how the system of medical imaging operates, to define its impact on the image quality and to know how to mitigate it in order to use the obtained image effectively.

## 1.3 Medical imaging techniques

### 1.3.1 Medical imaging

Medical imaging plays a vital part in illness diagnosis and detection. It has known a great progress in the recent years which led to a better diagnosis by narrowing the causes of disorder and offers new hopes for a better treatment of several diseases. The medical imaging basically relies on two specialties that include different types of medical imaging machines [6] [7]:

#### 1.3.1.1 Radiology imaging

It creates images by applying an external energy wave to a specific area in the body. It includes:

- X-ray: It uses ionizing radiation by sending beams that goes through the body and which will be mitigated by the bones, organs or tissues leading to have an image of that specific part.

- Sonogram: It is also referred as ultrasound and it involves the use of a liquid gel and a transducer probe that sends vibrations. These waves spread in the body and got reflected once hitting an obstacle.

- Magnetic resonance imaging (MRI): This technique is based on the phenomenon of hydrogen atoms resonance of water molecules in the human tissues when they are excited with a magnetic field, creating a signal that is detected and encoded leading to have a detailed image.

#### 1.3.1.2 Nuclear medicine

It develops images with internal radiation waves from inside the body with the use of small amounts of radioactive materials. It includes:

- Positron Emission Tomography (PET) scan: This is a tool that is commonly used to identify tumors in the body.

- Scintigraphy: It uses a very small amount of radionuclide (radioactive chemical) and a scanner to get where the radionuclide is captured resulting in an image.

### 1.3.2 Medical imaging history and evolution

Doctors were relying on their perception in order to diagnose the patients before the invention of diagnostic equipment and they sometimes needed surgery to identify the problem and give the affected person the right treatment. Then, in 1895, the German Physicist Wilhelm Conrad Röntgen discovered the X-ray [8] and paved the way to the appearance of the medical imaging field. After some experiments, in 1896, he succeeded to produce an image of his wife's left hand and this technique became common.

Figure 1.1: The first X-ray of Röntgen wife's [8].

In the early fifties, the nuclear medicine has known an evolution with the appearance of scintigraphy and positron emission tomography (PET) [9]. Then in the mid-fifties, the father of the echocardiography Inge Edler that is a Swedish cardiologist performed the first ultrasound [10]. After that, in 1972, two British radiologists Allan McCornack and Godfrey N. Hounsfield invented the scanner [11] and they were awarded the Nobel Prize in 1979. In the same year, the first MRI image was conducted on an animal by the American chemist Paul Lauterbur [12]. This following figure presents some images obtained from some medical imaging tools.

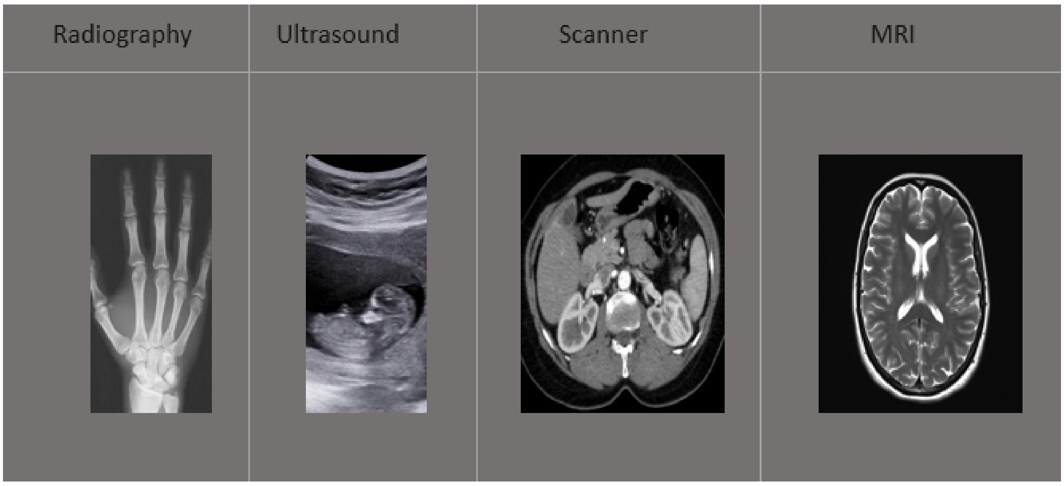


Figure 1.2: Results from different medical imaging tools [13] [14] [15]

Since the discovery of X-ray, more than 120 years ago, medical imaging has immensely progressed and this improvement is in the favor of humanity. In fact, patients can have an early and effective diagnosis in the case of some diseases.

In our research work, we will focus on MRI as a medical imaging technique and we need to go deeper and understand how does it work and what are its limits in order to overcome these challenges.

## 1.4 Magnetic Resonance Imaging (MRI)

A Magnetic Resonance Imaging (MRI) scan is an examination that allows doctors to see within the body in two or three dimensions. Many organs, such as the brain, spine, and heart, may be studied with extreme precision. It is commonly used in neurology to see the brain's structure and tissues. Hence, it provides information that cannot be obtained using x-rays, ultrasounds, or scanners.


Figure 1.3: Magnetic Resonance Imaging device [16].

Understanding the principles that underlie this imaging modality and its different applications can help doctors grasp the benefits and drawbacks of its use, which can help them make better decisions for patient's treatment.

### 1.4.1 MRI principle: Nuclear Magnetic Resonance

MRI is adapted from one of the main analytical techniques used in chemistry, the principal of Nuclear Magnetic Resonance (NMR). The NMR phenomenon was first described experimentally by both Bloch and Purcell in 1946, for which they were both awarded the Nobel Prize for Physics in 1952. Then, the first clinical MR images were produced in Nottingham and Aberdeen in 1980 [17].

After years of progress and evolution, MRI has become a widely available and powerful clinical tool. It is based on the observation of water protons. In fact, when water molecules are exposed to radio waves and the magnetic field created by the MRI device, they emit electromagnetic waves [18]. That is when the MRI machine records these waves with high accuracy and uses them to produce detailed images. These are the steps inspired from NMR, but there is a difference between these two techniques. In fact, NMR uses the frequency of the emitted radiation to create a spectrum of light whereas MRI uses the intensity of radiation coming from various areas of the body to create detailed images.

In order to dive deeper and understand more in details the physical phenomenon behind the MRI technique, we need to list the steps of NMR [19]:

1. Rest
2. Polarization
3. Resonance
4. Relaxation

In the case of MRI, each water proton is considered as a magnet that has a magnetic moment $\vec{u}$. In living matter, with the absence of an external magnetic field, each proton's magnetization has a random orientation, thus, the **rest** state can be represented by the sum of magnetic moments which is equal to zero $\vec{M} = \sum v.\vec{u} = \vec{0}$. During, the **polarization** phase, the protons are immersed in a magnetic field $\vec{B}_0$ , as a result, their spin magnetic moments $\vec{u}$ align locally with $\vec{B}_0$ direction. At this stage, the spins become animated with a rotational motion around $\vec{B}_0$ at a precise frequency which is directly dependent on $\vec{B}_0$ (frequency of Larmor). The next step is when we apply a radio frequency wave $\vec{B}_1$ where its frequency is equal to the frequency of Larmor. This is the condition of **resonance**. This radio frequency wave will disturb the balanced state of the protons as shown in the following figure.

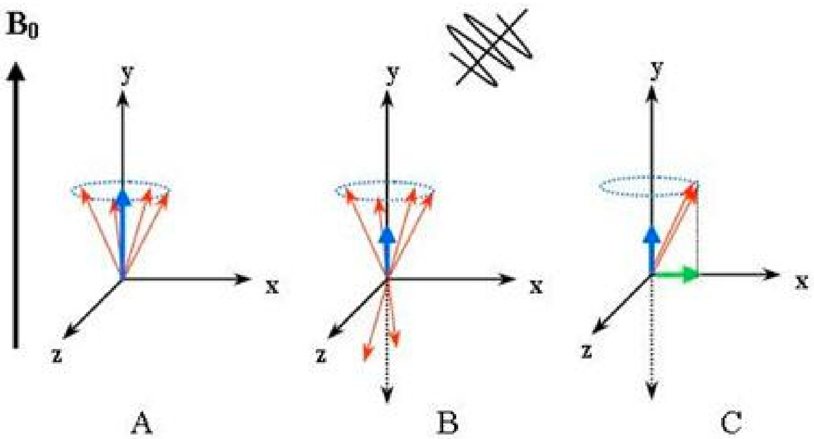


Figure 1.4: (A) Polarization state : rotational motion around ($\vec{B}_0$ ). (B) Application of radio frequency wave. (C) Protons balance state disturbed[20].

Once the radio frequency wave pulse stops, the **relaxation** phase is triggered. At this moment, an electromagnetic wave is emitted when returning to the balanced state and it can be measured using a radio frequency coil in order to create the MRI images.

### 1.4.2 Main components of MRI system

MRI system is mainly composed of four components which are the magnet, the gradient coil, the radio frequency (RF) coil and the computer [17]. The figure below presents these components.

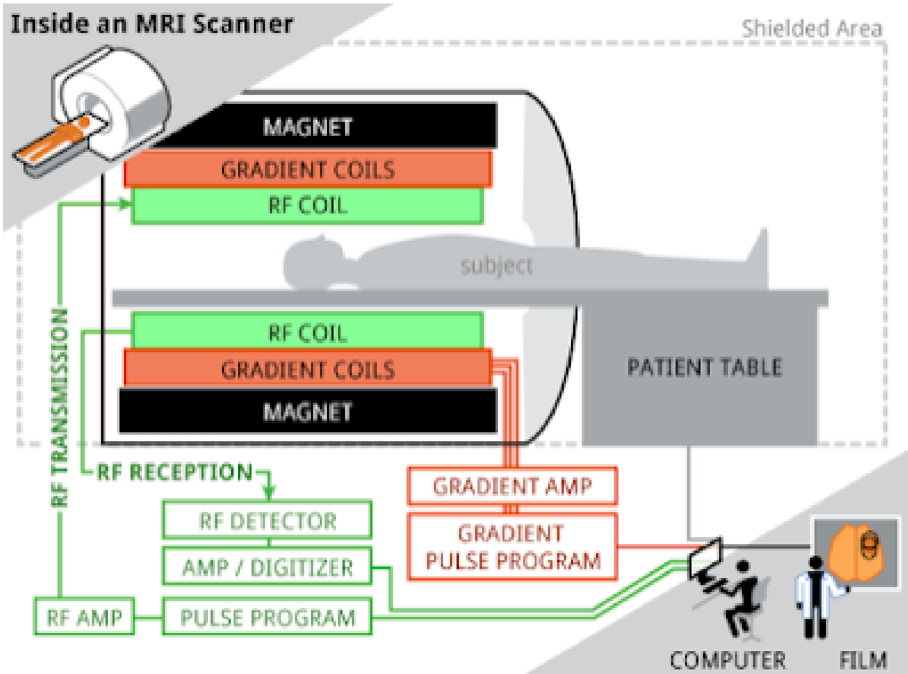


Figure 1.5: Main components of MRI system [21].

- The magnet plays a crucial role in the MRI system operation. It produces the main magnetic field called $\vec{B}_0$ which has to be stable and very intense.

- The gradient coils are used to create controlled variation in the primary magnetic field.

- The communication link is the radio frequency (RF) coil which is utilized for both signal transmission and reception with patient's body in order to create an image.

- An MRI image is created and displayed through series of particular steps that must be handled by the computer. It takes in charge all the acquisition and processing control.

### 1.4.3 MRI images acquisition

The MRI system allows to obtain digital images in three dimensions of the cortex, white matter (WM), and cerebrospinal fluid (CSF), etc. [22] However, two parameters that can be varied are involved in the acquisition:

- **Repetition Time (TR)** which is the amount of time between subsequent pulse sequences delivered to the same slice.

- **Time to Echo (TE)** is the delay between the delivery of the RF pulse and the reception of the echo signal.

Different images can be created when varying the TR and TE. T1-weighted end T2-weighted scans are the most frequent MRI sequences. Short TE and TR times are used to create T1-weighted images. The T1 properties of tissue are primarily responsible for the image's contrast and brightness. The figure below presents a T1-weighted image.

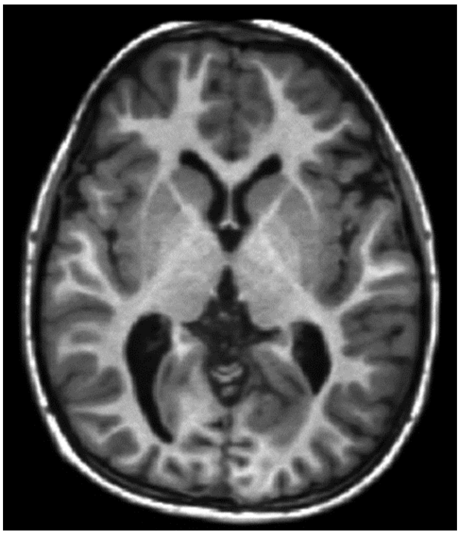

Figure 1.6: T1-weighted image [13].

On the other hand, T2-weighted images are created by employing long TE and TR times. The T2 characteristics of tissue are primarily responsible for the contrast and brightness in these images. The following figure shows a T2-weighted image.

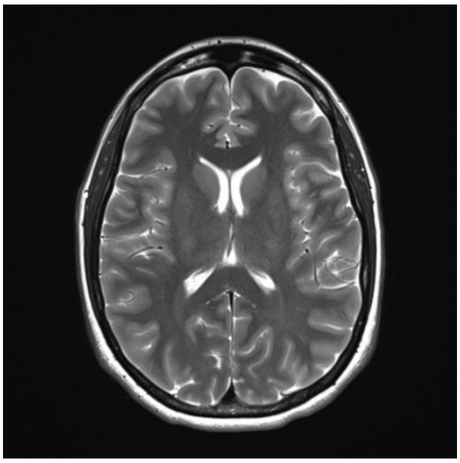

Figure 1.7: T2-weighted image [13].

The Fluid Attenuated Inversion Recovery (FLAIR) is the third frequently used sequence. The Flair image is comparable to a T2-weighted image, but the TE and TR times are significantly longer. In this sequence, it is much easier to distinguish between CSF and an abnormality because the CSF fluid is attenuated and darkened and the abnormalities remain visible. The figure below presents a FLAIR image.

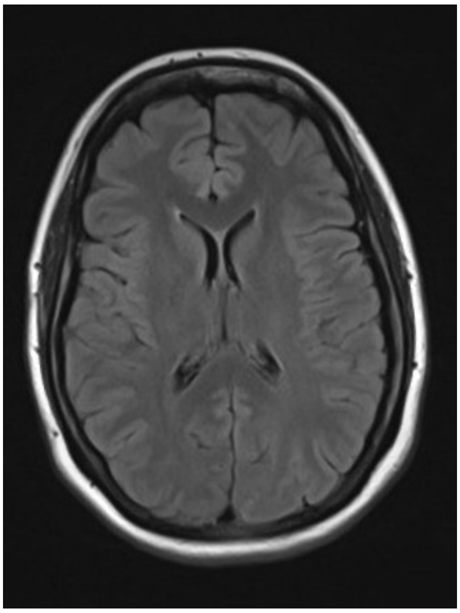

Figure 1.8: FLAIR image [13].

Finally, when the TR time is long and the TE time is short, the obtained image is called Proton Density acquisition (PD) as shown in the figure below.

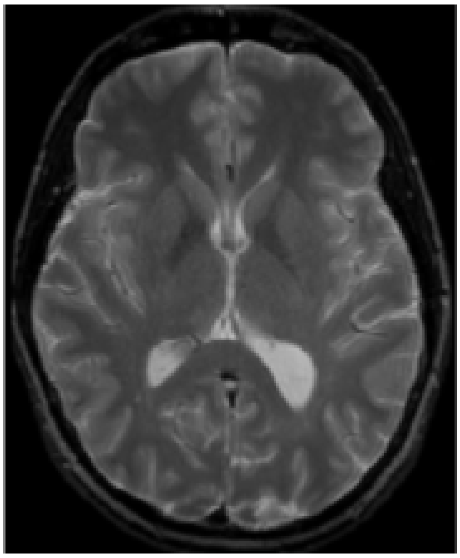

Figure 1.9: Proton Density [13].

The advantage of MRI is that it allows you to see the anatomy in all three planes: axial, sagittal and coronal as shown in the following figure.

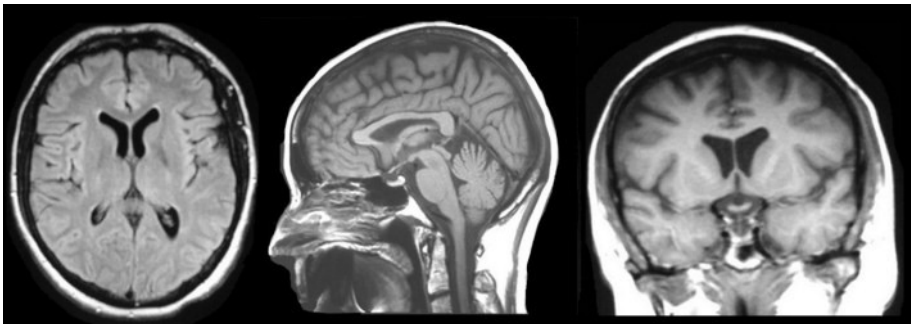

Figure 1.10: Images in all three planes : axial, sagittal and coronal [13].

### 1.4.4 MRI types of imperfections

The sources of imperfection in MRI are numerous. It can be caused by an image encoding error, artificial loss or enhancement of a signal, etc. These artifacts can cause image distortion to the anatomical image or it can simulate a pathological process [23] leading to a possibility of patient's misdiagnosis. That is why, it is highly important to identify the sources of imperfections in order to have a better understanding. Hence, we will be able to minimize or even eliminate their effects.

#### 1.4.4.1 Noise

The presence of spurious information that is randomly added to the image details is known as noise. It is an artifact that appears as a grainy structure which covers an image and takes various shapes and looks, but it will always remain a distracting information that decreases the image quality. The Signal to Noise Ratio (SNR) is commonly used to assess noise disruption. It is mainly visible in darkened areas where the SNR is low. As a result, the sharpness of the image details is lost [18]. The following figure present a noisy MRI image in which we can notice the noise amount especially in the darkened areas.

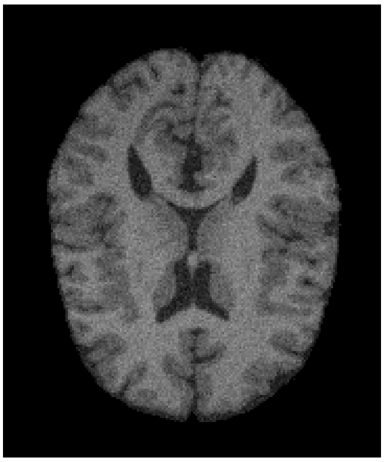

Figure 1.11: Noisy image.
Source: BrainWeb dataset.

The MRI image noise can be caused by the measurement chain (gradient coil, analog to digital converter, etc.) or even because of the patient. From that point, we can notice that noisy images are most likely obtained. That is why, we need a robust tool that can handle this artifact for better further diagnosis.

#### 1.4.4.2 Motion artifacts

One of the most commonly encountered imperfections is the motion artifact. It occurs when the analyzed segment undergoes a translation in space during acquisition. There are two types of motion [24]:

- **Periodic movements:** These are the movements of respiration, heartbeat and flowing blood, etc.

- **Aperiodic movements:** These are the patient's movements, eye movements, swallowing, etc.

These two types of movements result in the dispersion of the signal, thus obtaining a blurred image of the moving structure.

#### 1.4.4.3 Intensity non-uniformity

The differences in intensity recorded for the same tissue causes the intensity non uniformity. It is the smooth intensity variation [25] and it can be caused by different factors such as [26] [27]:

- The non-uniformity related to the imaging tool caused by the heterogeneity of the static field ($\vec{B}_0$ ) and the applied magnetic field for excitation ($\vec{B}_1$ ).

- Sensitivity of non-uniform reception coils.

- The non-uniformity related to biological properties of the tissue caused by different histological compositions of the tissues and the magnetic susceptibility artifact.

#### 1.4.4.4 Other artefacts

The artifacts presented previously can often be corrected in post-processing step. However, there are other imperfections disturbing the acquisition and it is difficult to correct them in post-processing. Among these artifacts, we can list:

- Because of the interaction between protons and their environment, the chemical shift artifact will occur. It causes misleading edges to appear, but it is not very seen in brain imaging.

- The discrete inverse Fourier transform will cause the truncation artifact to occur which causes an alternating band of hypo signal and hypersignal bands.

- The aliasing artifact which is a folding imperfection of the structures will occur due to the size of the field of view during acquisition.

## 1.5 Brain and MRI segmentation

The brain is the human body's control center. It manages everything we do and it is involved in every aspect of our lives whether we are thinking, dreaming, or doing a physical activity. It is a state of art of engineering in which many pieces are joined together in a specific way. Each part of the brain is responsible for a specific function, making it the ultimate processor. That is why, in order to diagnosis disorders, we have to understand the brain anatomy.

### 1.5.1 Brain anatomy

The brain is mainly composed of three structures the brainstem, cerebellum and cerebrum [28] as shown in the figure below.

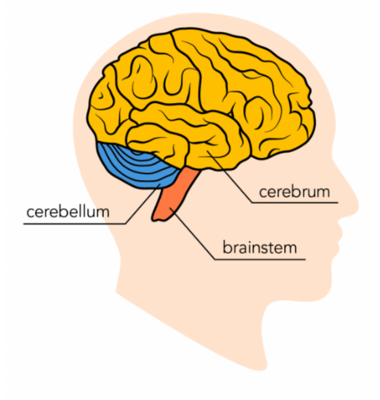


Figure 1.12: Main three brain structures [29].

- The brainstem connects the cerebrum and the cerebellum to the spinal cord as a relay center.
- The cerebellum is responsible for keeping muscle motions coordinated and maintaining balance.
- The cerebrum is the largest component of the brain. It is responsible for higher functions such as touch, vision and hearing interpretation as well as speaking, learning and motor behavior control. In turn, it is divided into two hemispheres, left and right.

The cerebrum is covered by the cerebral cortex which is divided into four lobes which are the frontal lobe, temporal lobe, parietal lobe and occipital lobe. Besides, the cerebrum involves the limbic system that contains structures such as the hippocampus and the amygdala. This system is involved in processing memories and emotions. The following figure shows the different parts of the brain including lobes and other structures.

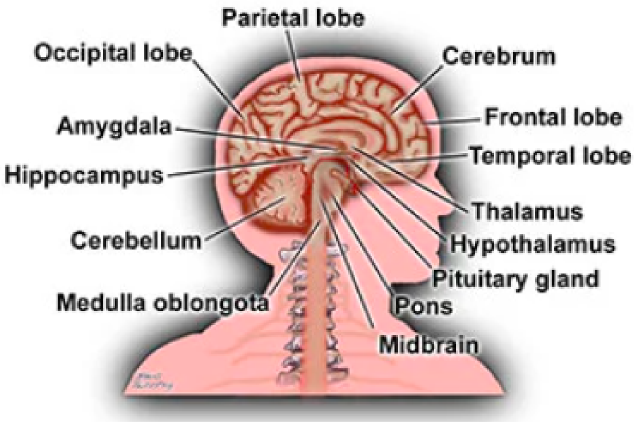


Figure 1.13: Brain anatomy [30].

We previously presented the brain in term of anatomical structure. Diving deeper in details, we find that another common divider exists which is the separation of the brain's gray and white matters.

- Gray Matter (GM) is mainly the spherical structure that contains the neuronal cell bodies and their dendrites. It is the area where the processing is done.

- White Matter (WM) refers the brain and spinal cord parts that are responsible for communication between gray matter areas as well as communication between gray matter areas and the rest of the body. It is like a pathway.

Finally, another part of the brain that is important and must be mentioned is the cerebrospinal fluid (CSF). It covers the brain and the spinal cord and play the role of a protector. These structures and parts are highly important when it comes to diseases diagnosis and illness prediction.

### 1.5.2 Brain MRI segmentation

Several levels of description can be selected when we perform a brain MRI images segmentation. This selection depends on the area of interest in a given application:

- According to the tissue present in each pixel: in this case, three matters are essentially taken into consideration, namely the gray matter, the white matter and the cerebrospinal fluid.
- According to the cerebral structure or the region of this structure that pixel contains in majority: in this case, we are mainly seeking to delimit the cortex and the central nucleus or to discriminate the CSF present inside the cortical sulci from the ones present in each of the ventricles.

The presence of artifacts in the acquisition process complicates the image segmentation in both cases.

### 1.5.3 Challenges and objectives

We previously mentioned the importance and the functions of the gray matter (GM), white matter (WM) and the cerebrospinal fluid (CSF) in the brain and the nervous system. However, several studies conducted by neuroscientists have proven the relation between GM, WM and CSF and neurological diseases [31]. And an early diagnosis or prediction of that disorder will allow the affected person to get a better treatment and thus a high cure rate. As a result, MRI images analysis is mandatory.

Image segmentation and classification present the key process helping in image analysis, comprehension and interpretation. A traditional approach consisting in manual segmentation is still employed in some cases. But it is a time consuming that needs high level of precision and it sometimes yields non-reproducible results [32]. As a result, brain data needs to be segmented using semi or fully automatic segmentation algorithms. The primary MRI brain segmentation methods focus on grouping the brain into three regions which are GM, WM and CSF. Segmentation of the total brain into these regions has been one of core challenges for the past two decades and it remains an active area of research. However, due to the poor signal to noise ratio as well as the presence of other artifacts in the MRI raw data, brain MRI segmentation (BMS) is challenging and needs numerous pre-processing and post-processing steps.

From our point of view, it is still difficult to have one generic solution that can overcome all the artifacts together. Thus, it would be interesting to combine existing techniques in order to find an efficient segmentation and classification solution. From that point, the main objective of our master thesis is to design and develop an efficient solution that is capable of performing the brain MRI segmentation and classification with the presence of previously mentioned artifacts.

## 1.6 Conclusion

In this chapter, we introduced some essential elements associated with our work context. First of all, we presented the clinical motivation where we listed some neurological disorders that increase the importance of an effective diagnosis for a better treatment. Secondly, we mentioned different medical imaging techniques, the evolution and the history of this field. Thirdly, we explained the principal of MRI and its main components. Besides, we introduced MRI images acquisition and the existing imperfections that affect the analysis process. Finally, we emphasized the necessity of a tool that is able to overcome the problems related to the image quality and performs the segmentation and the classification of brain tissues in MRI images. In the following chapter, we will present the different state of the art segmentation methods of brain MRI images as well as data fusion theoretical background.

# Chapter 2

# Theoretical Background and State-of-the-Art

## 2.1 Introduction

In this chapter, we will provide an overview of the different techniques of MRI images segmentation as well as the data fusion approach. First of all, we will provide a classification of the different approaches and methods related to brain MRI images segmentation and their background. Then, we will present the state-of-the-art methods. Finally, we will explain the representation of information uncertainty as well as data fusion approach and how it is applied in both probabilistic and evidential fields.

## 2.2 Overview of Brain MRI Segmentation and Classification methods

Segmentation consists in splitting an image into segments that have high correlation with areas of interest in the image. The purpose of this technique is to make an image more meaningful and easier to analyze by simplifying or changing its representation [33]. However, because of the complexity and the inaccuracy in the case of medical images analysis, not all the methods can be employed.

The figure 2.1 presents a diagram containing the main MRI images segmentation methods: edge-based methods, region-based methods and hybrid methods. As shown, image segmentation methods are classified based on two criteria which are discontinuity and similarity [34]. Edge-based methods are those based on discontinuity and region-based methods are those based on similarity whereas the hybrid methods combines both criteria.

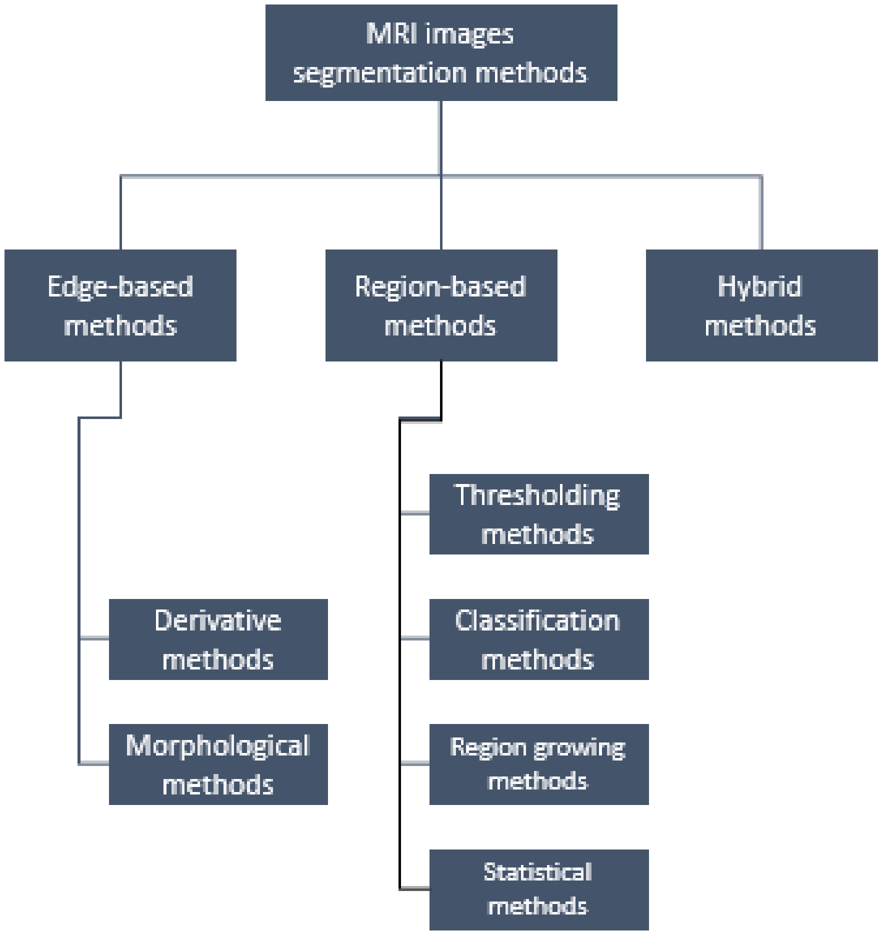


Figure 2.1: Different image segmentation methods.

## 2.2.1 Edge-based methods

Edge detection is a branch of image processing and computer vision research that focuses in particular on feature extraction [35]. It is a basic step in the image segmentation process. Its purpose is to find object boundaries within images by identifying brightness discontinuities or sudden changes in the image intensity [36].

In these methods, The detection of an image's boundaries dramatically reduces the amount of data. Thus, it eliminates information that can be considered less relevant while maintaining the important structural properties. Edge detection can be performed in many ways. However, the majority of methods can be grouped into two categories: derivative methods (first and second order) and morphological approach [37] [38].

#### 2.2.1.1 Derivative methods

Derivative methods are gradient and Laplacian which are based edge detection methods. Gradient methods identify locations of large intensity changes by searching the maximum and minimum in the first derivative of the image. Several operators are used by this approach, i.e., Sobel, Prewitt, ...etc. The Laplacian methods look for zero crossings in the second derivative of the image in order to detect boundaries [38], these methods include difference of Gaussian and the Laplacian of Gaussian (e.g., Marr-Hildreth method). In practice, in order to employ the optimal derivative edge detection methods, we should identify the edge model of the objects to be detected. Indeed, there are four main types of edges as shown in the figure 2.2.

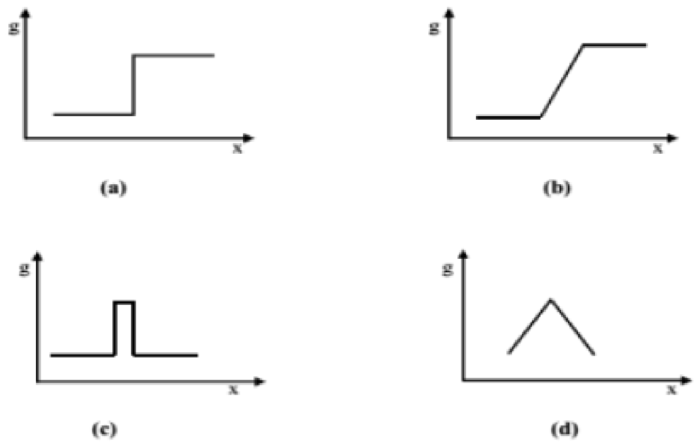


Figure 2.2: Edge Types : (a) Step Edge (b) Ramp Edge (c) Line Edge (d) Roof Edge.

#### 2.2.1.2 Morphological approach

The morphological operators work on each pixel's local neighborhood. The structuring element represents the shape of the neighborhood [39]. Besides, it can have various sizes and shapes. The commonly used structuring elements are the isotropic and the square. Among the morphological operators, we can list:

- **Dilation:** It returns a structure that has a larger shape compared with the original one.
- **Erosion :** It removes particles smaller than the used structuring element as well as the possibility of huge particles separation.
- **Opening :** It consists in an erosion followed by a dilation. It removes the particles whom size is smaller than the structuring element and separates large particles.
- **Closure :** It is a dilation followed by an erosion that removes small holes and connects nearby structures.

The figure 2.3 presents an original image on which we performed dilation and erosion and after that, we combined them together in order to produce an opening and a closing.

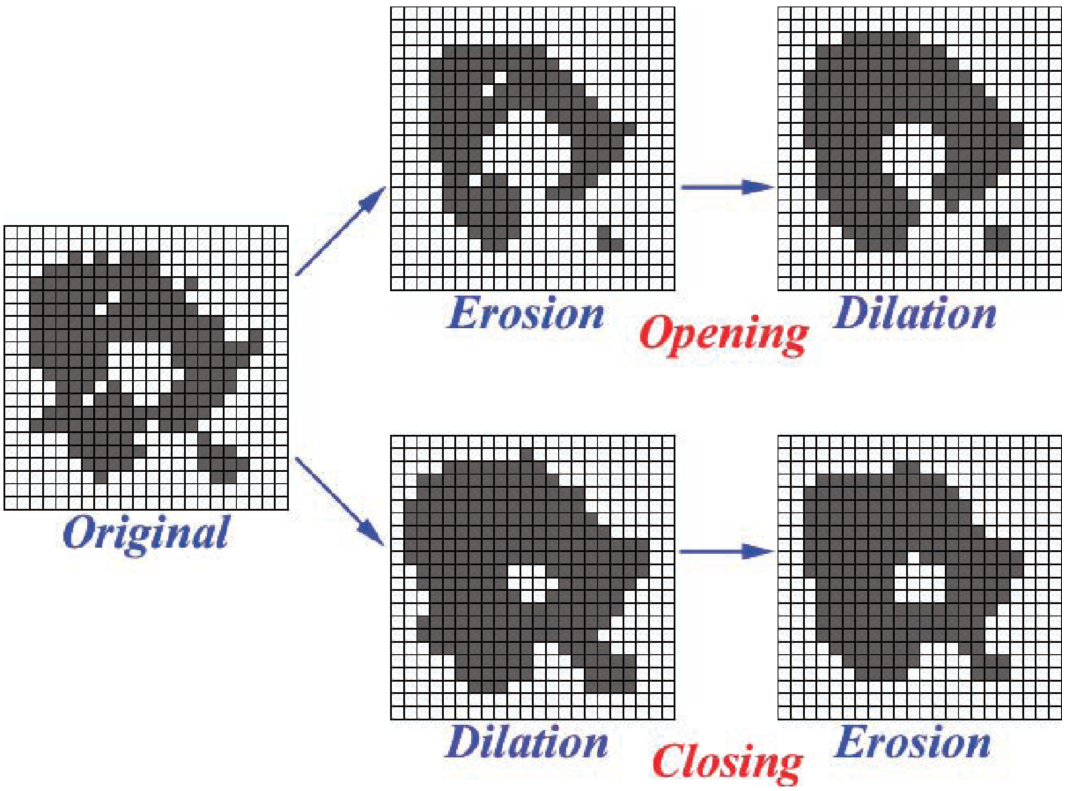


Figure 2.3: Morphological methods [40].

### 2.2.2 Region-based methods

On the one hand, an edge based method tries to investigate the boundaries of an object before discovering the object itself. On the other hand, region-based method may begin in the object's inside and then grows outward until it encounters the boundaries of the object [41]. There are various region-based methods and they can be classified into four categories which are thresholding, classification, region growing and statistical methods.

#### 2.2.2.1 Thresholding methods

Thresholding is one of the most used techniques for images segmentation. It considers that the image is made up of regions with varying gray levels. In fact, it determines an intensity value referred to as the treshold, that distinguishes the desired regions [42]. All pixels with an intensity between two thresholds are grouped into one class. This method is basically dependent on a good threshold identification. Thus, once failing to fulfill that, we can end up with a inappropriate segmentation and poor results. Thresholding is usually employed in the first steps in an image processing cycle.

Thresholding is a simple and a fast segmentation method and it is frequently used for medical images preprocessing step [43]. However, it ignores the spatial information of an image. Therefore, this technique is vulnerable to noise and intensity non-uniformity which are common in MRI images.

#### 2.2.2.2 Region growing

Region growing is a technique used for linked region extracting of an image using some predefined criteria [33] which can be based on image edges or intensity information. This technique requires a seed point that is selected manually and it extracts all pixels linked to the initial seed with intensity value. The first step of region growing starts with pixels known as seeds belonging to the structure in focus. In the next step, local neighborhood region pixels are inspected and added to the growing region based on the homogeneity criterion. This step will be repeated until no more pixels can be added to the growing regions. At the end, all new pixels in the growing regions are used to display the object [44]. Region growing is frequently employed as part of a larger set of image processing operations.

In order to determine the seed point, the need of manual interaction is considered as the main disadvantage of this technique. It also can be noise sensitive, causing the appearance of holes in the extracted region or it can even become disconnected [33].

#### 2.2.2.3 Statistical methods

When an image has a random structure, it can assume to be the result of stochastic process driven by computer parameters from the image itself. This is the principle of methods based on Markov random fields which is a popular way for modeling the images texture and expressing the spatial interaction carried by pixels. In fact, the pixel's neighbors have a high probability of belonging to the same class as the pixel itself. In this approach, a conditional distribution is used to express the mutual influence of pixels in a particular image.

#### 2.2.2.4 Classification methods

Classification methods allow to group objects in more homogenous classes. Thus, the obtained objects in the same group have a lot in common and it becomes easy to distinguish the different objects [41]. We will address two types of classification : Supervised and unsupervised classification.

a) **Supervised Classification**

Supervised classification methods assume the a priori knowledge of the membership of each sample of the training set to a given class, which is the same as assuming an a priori knowledge about the image to be segmented [45]. In the case of medical MRI brain images, the supervised classification of these images requires the creation of a learning set for each class which is a difficult task even for experts. Therefore, we are interested in unsupervised methods in the field of Brain MRI images segmentation. The figure 2.4 shows an example of segmentation based on the supervised classifier Support Vector Machine SVM for brain tumor detection.

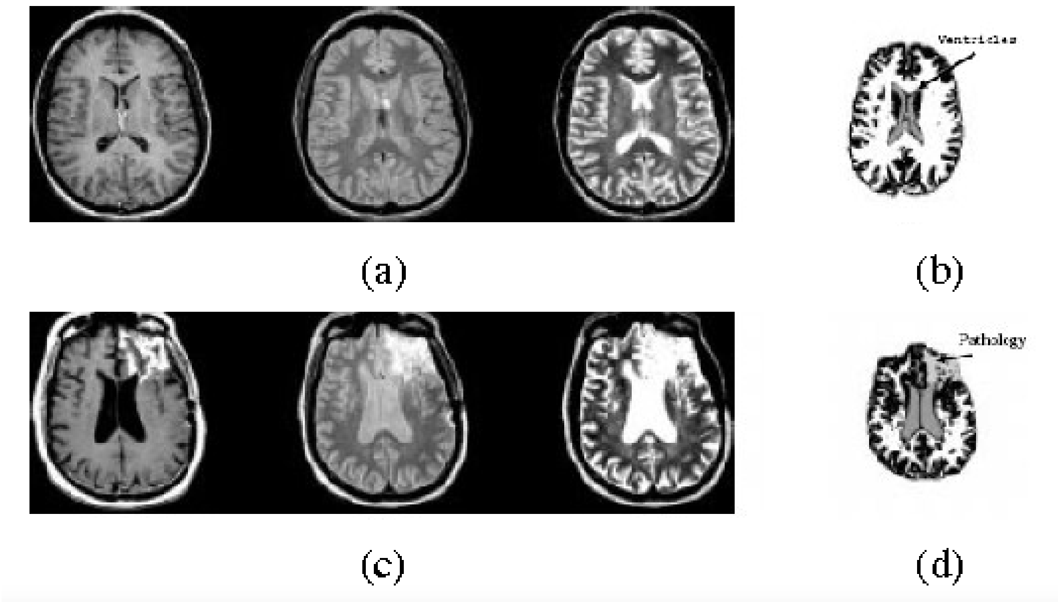


Figure 2.4: (a) T1-weighted, PD and T2-weighted images of normal slice from left to right (b) after segmentation (c) T1-weighted, PD and T2-weighted images from an abnormal slice from left to right (d) after segmentation. White=white matter; Black=gray matter; Dark Gray=CSF; Light Gray=Pathology in (b) and (d) [46].

b) **Unsupervised Classification**

The unsupervised classification methods perform a blind classification and thus perform a segmentation without having any a prior knowledge of the image. The clustering methods such as K-means and Fuzzy C-means are the most widely used in the case of MRI brain image segmentation. Besides, clustering algorithms do not require training data, but they need an initial segmentation. Then, they iterate between segmenting the image and giving representative properties to define each class. From that point, we can say that clustering methods use the available data as a training set.

We can obtain poor results using clustering methods in case the used attributes do not represent each class very well. These methods can also be sensitive to noise and intensity inhomogeneity. Therefore, many pre-processing and post-processing steps should be employed to overcome these challenges.

### 2.2.3 Hybrid methods

Each one of edge-based and region-based methods of segmentation has a set of strengths and weaknesses. For example, noise can affect edge-based methods more than region-based methods. The purpose of hybrid methods is to combine these two approaches trying to cover the weaknesses and to emphasize the strengths of each one [47].

## 2.3 State-of-the-Art on brain MRI Segmentation Methods

Due to the variety and complexity of images, image segmentation is one of the most challenging tasks in image analysis and interpretation and computer vision. It consists in dividing an image into different non-overlapping and consistent parts according to the need of various application. In medical field and more precisely in MRI brain images analysis field, the segmentation process consists in separating different brain regions for a specific reason such as tumor detection, structural changes analysis for disease prediction, ...etc. This work can be manually done, but it remains a difficult task having a high error rate. However, it is important to decrease the error rate and go towards robust and accurate results by automating this task with the use of segmentation algorithms. Therefore, several segmentation methods have been proposed for this purpose and yet it is still challenging to overcome all the encountered artifacts such as noise and intensity non-uniformity that are likely occurring in the case of MRI images. In this section, we will present different state-of-the-art methods that can be used in brain MRI images segmentation.

We previously classified segmentation methods based on two features which are discontinuity and similarity where we defined edge-based methods, region-based methods and their combination to obtain hybrid methods.

Starting with edge-based, in the state-of-the-art methods based on this approach, edge detection and filtering techniques are usually used in the pre-processing and the post-processing steps of the whole segmentation process in order to accurately preserve some edge information. Motivated by this idea, Zotin, Alexander, Konstantin Simonov, Mikhail Kurako, Yousif Hamad, Svetlana Kirillova. [48] proposed a solution for edge detection in MRI images based on Fuzzy C-means (FCM) clustering algorithm. First, they used the Balanced Contrast Enhancement Technique (BCET) to improve the quality of medical images by removing noise. After that, using FCM image segmentation is performed. Finally, they used Canny edge detector in the post-processing step in order to detect the image's edges. Their technique produced better results by preserving more edge information with greater accuracy.

Moving to region-based segmentation which is in its turn divided into several categories. Firstly, in 2018, in the context of threshold based methods, Maolood et al. [49] developed a new medical image segmentation solution for cancer based on fuzzy entropy and level set algorithm. The analysis was conducted on three types of medical images including brain MRI and the experimental results show that the proposed method's compact constraint is effective and it showed better results than other segmentation algorithms. In region growing-based methods, in order to overcome MRI image segmentation challenges, Chidadala J., Maganty S.N., Prakash N [50] introduced an automatic seeded point selection region growing algorithm with a clustering technique. The image is firstly preprocessed using a median filter before being segmented using automatic seeded point region growing algorithm. At the end, the image classification is performed using a support vector machine (SVM). Going to statistical methods, Ahmadvand A., Yousefi. S.,M. T. Manzuri Shalmani [51], proposed a novel method using a proper combination of the Markov Random Fields (MRF) model and the watershed algorithm to address and overcome the MRF weaknesses. The results show that the proposed method is effective in MRI images and significantly reduces computational time which is important in online applications.

The last category that we have mentioned in region-based approach is classification-based methods which are divided into two subgroups; the supervised and the unsupervised classification. In the first group, Ahmed Kharra A.t, Neji. M [52], presented a 3D CNN architecture for brain tumor segmentation. The results show that the proposed solution is promising and performs very well. Moving to the second group; the unsupervised classification that includes clustering which is the most popular technique.

Clustering is widely used in medical images segmentation and more precisely in MRI brain images segmentation. There are many clustering algorithms such as K-means and Fuzzy C-means (FCM) algorithms. In k-means, data is only included in one cluster. In fact, it is a hard clustering algorithm. Whereas, in FCM data have different degrees of membership to the clusters and it can be included in all the existing clusters [53] as it is a soft clustering algorithm. Thereby, FCM is more suitable to deal with incomplete and uncertain information and it has more tolerance to ambiguity. Indeed, several comparative studies between the two algorithms were conducted in the field of medical images segmentation that were in the favor of FCM in terms of accuracy and more information perseverance [53].

FCM was firstly proposed by Bezdek [54] and as we previously mentioned FCM is tolerant to ambiguity. It is efficient in the segmentation of images having simple texture and background. But since it only considers gray-level information while ignoring spatial information, it showed poor results with images having complex texture and background and even with images corrupted by noise. In order to tackle this problem, the most common solution is including local spatial information in an objective function to improve the segmentation process. Inspired by this idea, Ahmed et al. [55], introduced the FCM algorithm with spatial constraints (FCM S). In this proposed solution, the traditional FCM's objective function is adjusted to take into consideration the intensity non-uniformity and to allow the influence of a pixel labeling by the labels in its local neighborhood. Unfortunately, FCM S is time consuming because of its computational complexity because of computing the spatial neighbors' term in every iteration. That is when, Chen and Zhang [56], reduced the execution time of FCM S by using a mean and median filtering to get the spatial neighborhood information in advance. They proposed two variants FCM S1 and FCM S2 with lower computational complexity than FCM S. However, neither FCM S1 nor FCM S2 are robust in the presence of noise.

Another outstanding algorithm in terms of execution time is Enhanced FCM (EnFCM) [57] which carries out clustering based on gray level histograms rather than pixels of summed image. However, EnFCM still do not produce good results in presence of noise. Cai et al. [58] introduced the fast generalized FCM algorithm (FGFCM) starting from EnFCM with the purpose of ensuring noise immunity and detail preservation. FGFCM can increase FCM's robustness and computing efficiency to some level, but it requires more parameters than FCM. Moreover, Krinidis and Chatzis [59] developed the robust fuzzy local information c-means (FLICM) that is free of parameter selection. FLICM solves the problem of parameter selection but it is still not robust for local information in images.

In order to improve FCM to deal with noise and several artifacts, different other variant were also proposed such as kernel weighted fuzzy local information c-means (KWFLICM) proposed by Gong et al. [60] and neighborhood weighted FCM algorithm (NWFCM) introduced by Zhao et al. [61]. Following the same path of contributions, Tao Lei et al. [62], proposed fast and robust FCM which is a relevant FCM variant. FRFCM improves the noise immunity and detail preservation at the same time by using morphological reconstruction (MR). Moreover, instead of computing distance between pixels within local spatial neighbors and their clustering centers, FRFCM employs a faster membership filtering. Therefore, FRFCM is more robust than other FCM variants for noisy images and it has lower computational cost compared to FCM algorithms. But detail preservation still needs improvement.

In order to make better medical decisions, we need to increase the accuracy of the segmented image. That is why, the detail preservation have to be considered in the first place. This loss of information is due to several artifacts such as noise and intensity inhomogeneity which introduce the concept of uncertainty in a pixel membership. Thus, we need to find a good representation of this uncertainty in order to deal with it effectivelly leading to have better results. Furthermore, we are always trying to reproduce the human instinct and to simulate the way of thinking of the human brain in a formal way by developing automatic solution for segmentation and classification and as humans we always rely on several sources of information to deal with uncertainty and to make good decisions. Therefore, in addition to uncertainty representation we need to be able to perform data fusion in order to overcome the ambiguity in the given information.

## 2.4 Data Fusion Concept

Humans take into consideration several information in order to make a decision in the daily life. In fact, our brain combines various information to come up with a decision. For example, a doctor can take a medical decision based on the patient's state and examination and his/her knowledge by performing information fusion. Therefore, it is highly interesting to find mathematical models that can automatically perform data fusion in order to facilitate the analysis process and to improve the decision-making step.

The data fusion can be classified based on three different types as proposed by Durrant-Whyte [63]. The figure 2.5 illustrates this classification.

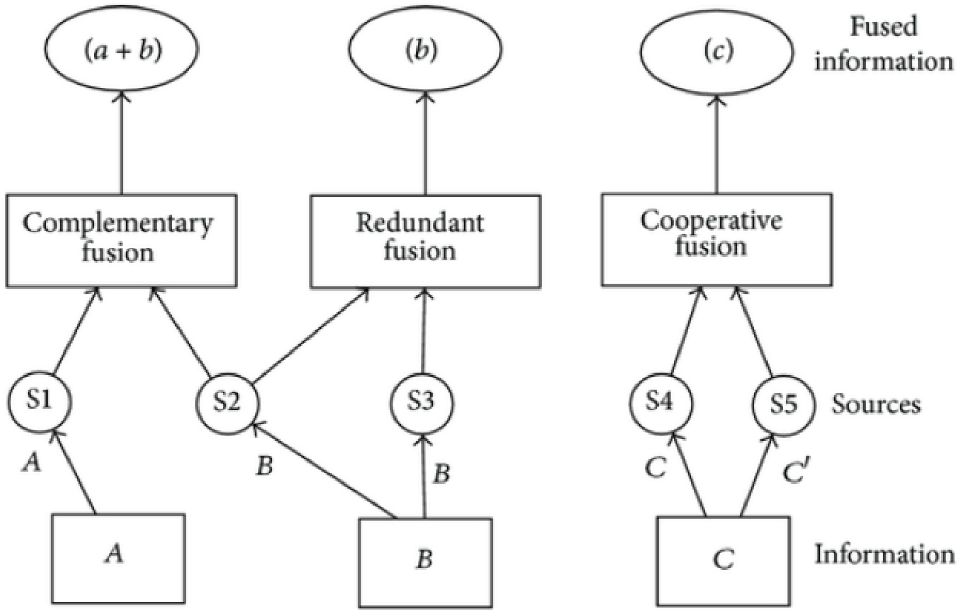


Figure 2.5: Data Fusion types [63]

- **Complementary fusion:** It consists in combining independent sources in order to give a complete information about the area of interest. Each source provides information from different part of that area.
- **Redundant fusion:** The fact of providing independent information of the same observed phenomena. This type of fusion increases the accuracy and the reliability.
- **Cooperative fusion:** Information are merged from independent sources where each source cannot provide the data measured by the other.

Theoretical foundations of data fusion were established in the 1960s by Zadeh, Shafer and Dempster. And nowadays, it is used in several field such as medical, space technology and robotics. In fact, it can be very useful in the decision-making process especially with the presence of uncertainty. Therefore, we need to present two theories allowing us to incorporate the representation of the uncertain and non-precise in order to introduce the data fusion approach in both theoretical frameworks.

### 2.4.1 Theoretical Background

Several theoretical frameworks are used to represent information in data fusion. Some use belief theory and others use the probability theory. We will briefly present the needed backgound from these two theories.

#### 2.4.1.1 Probability theory

Probabilities are still the most commonly used theoretical basis for the representation of uncertain data due to its antiquity. In fact, it started in the sixteenth century and it was completely developed in the beginning of 19th century [64]. A conditional probability distribution represents the relationship between the information in the data and the hypothesis being investigated and a Bayes ‘rule can be used to merge many probability distributions. The mathematical equation of Bayes ‘rule is [65]:

$$P(A|B) = \frac{P(B|A)P(A)}{P(B)} \tag{2.1}$$

Where:

- P(A|B) is the probability that an event A happens given B is true. It is also referred to as the posterior probability of A given B.

- P(B|A) is the probability that an event B happens given A is true. We can interpreted as the likelihood of A given B.

- P(A) and P(B) are the probabilities of A and B occurring.

#### 2.4.1.2 Belief theory

The mathematical belief theory has its roots back to 1967 when Glenn Shafer firstly introduced it as a new approach to represent uncertainty. It is also known as Dempster-Shafer Theory and it defines the lower and upper bounds of probability in order to describe the belief in hypothesis [66] and it is a generalization of the Bayesian theory and consists in the quantification of the belied attributed to observed facts.

The Dempster-Shafer theory (DST) is based on a mutually exclusive set of state $\Omega$ which is referred to as the frame of discernment. The belief theory defines mass function describing the amount of belief in a hypothesis H. Each member of the power set $2^{\Omega}$ is associated to a mass function as follow:

$$\begin{aligned} & m : 2^{\Omega} \rightarrow [0,1] \\ & \textstyle\sum_{H \subseteq 2^{\Omega}} m(H) = 1 \end{aligned} \tag{2.2}$$

The sets having a non-null mass values are called focal elements.

The lower bound of a hypothesis H probability is represented by the belief function bel as shown below:

$$bel(H) = \sum_{A \subseteq H} m(A) \tag{2.3}$$

It represents the belief devoted to a hypothesis H including all the subsets $A \subseteq H$.

The upper bound of a hypothesis H probability is represented by the plausibility function pl as shown below:

$$pl(H) = \sum_{A \cap H = \emptyset} m(H) \tag{2.4}$$

This function measures how well the source given information are not conflicting.

We can say that belief can be interpreted as a measure of minimum likelihood (pessimistic) of an event and plausibility as a measure of maximum likelihood (optimistic) of an event.

### 2.4.2 Fusion in probability theory and belief theory

The fusion process paves the way towards decision. We will firstly introduce the combination rule in both approaches and then we will explore the decision making process.

#### 2.4.2.1 Combination

Even though probability theory is more oriented towards an estimation purpose (finding a representative value from observed event), it is possible to perform a purely probabilistic fusion using the Bayesian fusion method represented in the following equation for two different observations $n_1$ and $n_2$ of an event $H_i$ [67]:

$$P(H_i|n_1, n_2) = \frac{P(H_i)P(n_1|H_i)P(n_2|H_i)}{\sum_{k=1}^{i} P(H_k)P(n_1|H_k)P(n_2|H_k)} \tag{2.5}$$

This is the most commonly used Bayesian fusion operator. But, there are other fusion operators proposed in literature.

In the case of belief theory, Dempster's rule of combination is introduced in order to combine two independent belief functions. The rule is presented as follows [68]:

$$\begin{aligned}
&m_1 \oplus m_2(\emptyset) = 0 \\
&m_1 \oplus m_2(H) = \tfrac{1}{1-K} \textstyle\sum_{A \cap B = H \neq \emptyset} m_1(A)m_2(B) \\
&Where: \\
&K = \textstyle\sum_{A \cap B = \emptyset} m_1(A)m_2(B)
\end{aligned} \tag{2.6}$$

#### 2.4.2.2 Decision making

Decision making process is as important as the fusion, it is the result of analysis and interpretation and in some cases it can be vital like medical decision.

When it comes to the probability theory the most frequently used technique of decision making is choosing the maximum of a posterior probability. Whereas in the case of DST, there are several decision-making methods used, the two mostly applied are the pessimistic and optimistic choices. On the one hand, the pessimistic one is when the decision is taken in favor of the set having the greatest plausibility. On the other hand, the pessimistic choice is when the decision is made in favor of the class having the greatest belief value [67]. Besides, we can also refer to machine learning for decision making based on training and learning process.

### 2.4.3 Comparative summary

The table 2.1 presents a comparison between both probability and belief theories by identifying their strengths and weaknesses.

| Theory | Strengths | Weaknesses |
|---|---|---|
| Probabilistic theory | • Dealing effectively with the presence of several information sources<br>• Simplicity | High memory requirements |
| Dempster-Shafer theory | • Decision-Based method<br>• Managing uncertainty effectively<br>• Proving good results even with less amount of data<br>• Powerful towards assigning uncertainty and ignorance to hypothesis<br>• Flexibility | Computational complexity |

Table 2.1: Comparative summary of probability and belief theories

## 2.5 Conclusion

In this chapter, we provided an overview of the different techniques of MRI images segmentation and we introduced data fusion concept. First of all, we provided a classification of the different approaches and methods related to brain MRI images segmentation and we explained their background. Then, we presented several state-of-the-art segmentation methods discussed in literature. Finally, we introduced the idea of data uncertainty representation and we presented the data fusion approach and the way it is applied in both probabilistic and evidential fields. In the next chapter, we will explain our proposed method of our research and justify the used techniques as well as presenting the obtained experimental results.

# Chapter 3

# Proposed Method and Results

## 3.1 Introduction

Brain MRI images segmentation and classification with accuracy is important for better diagnosis and even diseases prediction. As we have mentioned in the first chapter, there are several challenges that we need to overcome in order to get better results. Besides, in the second chapter, we explained several Brain MRI segmentation (BMS) methods and we presented the state of the art algorithms used in BMS with a focus on FCM variants. Over time, algorithms become more robust and accurate, but we still need better results. Therefore, in this chapter, we will introduce the used techniques in our proposed solution and we will describe our method. Finally, we will explore the experimental results.

## 3.2 Used techniques

In this section, we will present the techniques that we used in our proposed solution by adapting them to our research work.

### 3.2.1 Fuzzy C-means variants

Fuzzy C-means is a soft clustering algorithm that is widely used in Brain MRI segmentation. As we explained in the previous chapter, many variants of this algorithm were proposed to overcome its weaknesses and the significant and the most developed variant that we have mentioned is FRFCM. It improved both noise immunity and detail preservation at the same time. In our research work, we created a new method that uses both FCM and FRFCM. In this section, we will dive into more details by explaining the steps of each algorithm.

#### 3.2.1.1 FCM: The classic algorithm

In FCM, each image pixel presented by a data point will be assigned to all existing clusters on the basis of computing the distance between the cluster center and the data point. The closer that data is to the cluster center, the more likely it belongs to that center. FCM works on the minimization of the objective function defined as:

$$J_m = \sum_{i=1}^{n} \sum_{k=1}^{c} (\mu_{ki})^m \left\| x_i - v_k \right\|^2 \tag{3.1}$$

Where:

- n : Total number of data points.
- c : Clusters number.
- m : Fuzziness index.
- $\mu_{ki}$ : Membership of $i^{th}$ data point to the $k^{th}$ cluster center.
- $x_i$ : The $i^{th}$ data point.
- $v_k$ : The value of $k^{th}$ cluster center.
- $\left\| x_i - v_k \right\|^2$ : Euclidean distance between $i^{th}$ data point to the $k^{th}$ cluster center.

Let X=$\{x_1, x_2, ..., x_n\}$ be the set of grayscale image pixel values, V=$\{v_1, v_2, ..., v_c\}$ be the set of cluster center values and U=$(\mu_{ki})_{c*n}$ be the fuzzy membership matrix. When we employ FCM on a grayscale image, the algorithm steps are described as follows:

**Input :** The set of grayscale image pixels X, fuzziness index $m \in [1.5, 3]$ and number of clusters c.

1. Initialization step:

   We initialize the fuzzy membership matrix 'U' with random values where $\sum_{k=1}^{c}(\mu_{ki}) = 1$ and set a value to the minimal error threshold $\varepsilon$ .

2. We compute the centers values as follows:

$$v_k = \frac{\sum_{i=1}^{n}(\mu_{ki})^m x_i}{\sum_{i=1}^{n}(\mu_{ki})^m} \tag{3.2}$$

   and we compute the objective function using (3.1) equation:

$$J_m^{old} = \sum_{i=1}^{n}\sum_{k=1}^{c}(\mu_{ki})^m \left\|x_i - v_k\right\|^2$$

3. We compute the new fuzzy membership matrix:

$$\mu_{ki} = (\sum_{j=1}^{c}(\frac{\|x_i - v_k\|}{\|x_i - v_j\|})^{\frac{2}{m-1}})^{-1} \tag{3.3}$$

   and we compute the objective function using (3.1) equation:

$$J_m^{new} = \sum_{i=1}^{n}\sum_{k=1}^{c}(\mu_{ki})^m \left\|x_i - v_k\right\|^2$$

4. Repeat the steps 2 and 3 until the minimum 'J' value is achieved $\left\|J_m^{old} - J_m^{new}\right\| \leq \varepsilon$.

**Output:** The fuzzy membership matrix 'U' and the cluster centers 'V'.

#### 3.2.1.2 FRFCM: The significant variant

In FRFCM, the clustering proposed is not performed based on the distance between the cluster center and the data point, but on the gray level histogram. Besides, it aims to find the saddle point of a Lagrangian function obtained from the objective function that is defined as follows:

$$J_m = \sum_{l=1}^{q} \sum_{k=1}^{c} \gamma_l \mu_{kl}^m \left\| \xi_l - \upsilon_k \right\|^2 \tag{3.4}$$

Where

- $\mu_{kl}$ is the fuzzy membership of the $l_{th}$ gray value to the $k_{th}$ cluster.
- $\sum_{l=1}^{q} \gamma_l = n$ where n is the number of pixels in the image.
- $\xi$ is the image reconstructed by morphological reconstruction.
- q represents the number of gray levels in $\xi$.

The algorithm of RFRCM can be described as follows:

**Inputs:** The grayscale image, the cluster number c, the fuzziness index m, the size of the filtering window w and the minimal error threshold $\eta$.

1. Compute the reconstructed image $\xi$ using closing morphological reconstruction on the original image. Then, compute the histogram of the obtained image $\xi$.
2. Initialize the membership partition matrix $U^{(0)}$ randomly.
3. Initialize t = 0 which represents the loop counter.
4. Compute the cluster centers using:

$$\upsilon_k = \frac{\sum_{i=1}^{q} \gamma_l u_{kl}^m \xi_l}{\sum_{i=1}^{q} \gamma_l u_{kl}^m} \tag{3.5}$$

5. Compute the new membership partition matrix $U^{(t+1)}$:

$$u_{kl} = \frac{\left\| \xi_l - \upsilon_k \right\|^{\frac{-2}{m-1}}}{\sum_{j=1}^{c} \left\| \xi_l - \upsilon_j \right\|^{\frac{-2}{m-1}}} \tag{3.6}$$

6. Go to step 7 if $max\{U^{(t)} - U^{(t+1)}\} < \eta$, otherwise, set t = t+1 and repeat the steps 4 and 5.

7. Calculate the membership partition matrix U' that corresponds to the original image from the membership partition matrix corresponding to the fuzzy membership of gray values.

8. Implement median filtering on membership matrix U' to get U".

- **Output:** The partition membership matrix U" and the cluster centers.

### 3.2.2 Dempster-Shafer theory

We have briefly explained the basics of the belief theory also called Dempster-Shafer theory (DST), in the second chapter.

DST is a formal framework for plausible reasoning that takes all available evidences into account [69]. In fact, it expresses the possibility of occurring for each member of the set of hypothesis and their powerset. Therefore, it is more suitable to represent the uncertainty of information than the probabilistic approach. In fact, it is essentially a generalization of the Bayesian statistical theory. Besides, belief theory allows to combine evidence weights from multiple sources using Dempster's rule of combination which is an advantageous and flexible combination operator. The main purpose of this combination is to reduce the uncertainty through multiple sources combination.

In our research work, we proposed to represent the membership of pixels to different clusters using the belief theory rather than assigning probabilities. In fact, having a better uncertainty representation will be helpful in the decision making process which is an important step in MRI brain images segmentation. In addition, in MRI brain images, we can find several artifact such as noise and intensity non-uniformity leading to have overlapping structures especially in the edges and the little details of the image. These overlapping pixels represent the uncertain information. It is the main cause of decreasing accuracy in the results of segmentation methods. Moreover, having several representation of the same information allows to reduce uncertainty. At this point, the dempster's rule of combination will play its role in order to pave the way towards more accurate decisions.

To summarize, the belief theory will be employed in order have a better membership representation and to perform a redundant fusion to reduce uncertain information. Therefore, the decision-making process can provide accurate results.

### 3.2.3 Decision Tree

Classification is very useful for the data analysis and interpretation processes. Many algorithms are used in machine learning to perform this task such as decision trees, neural networks, ...etc. Among all, the decision tree (DT) is one of the most commonly used inductive method [70]. This approach uses the tree representation in which each leaf node represents a classification or decision and each branch node represents a choice between a set of options. It is created by dividing criterion according to a training dataset that has been recursively divided into two or more root nodes. Then, the process is repeated until a termination condition is met and the leaf nodes are reached. This method has several advantages and it is used in many real-world applications in varied fields such as biology and healthcare. In fact, it can easily handle continuous and categorical data to predict categorical classes.

Over years of research, researchers have proposed many decision tree algorithms that are able to handle different dataset. Among all, we opt for **CART** which stands for Classification And Regression Trees. As we mentioned previously, in the decision tree, the nodes are split into sub-nodes using a threshold value of an attribute. The CART algorithm does the same by looking for the best homogeneity for the sub-nodes. The root node is considered as the training set and is divided into two by considering the best attribute and threshold value. Moreover, this algorithm is non-parametric, so it does not rely on information from a certain type of distribution. Besides, outliers in the input variables can not have an important impact on CART and that is why this algorithm does not require a huge data preparation. Furthermore, CART can use the same variables more than once in different parts of the tree. Thanks to that, it can uncover complex inter-dependencies between sets of variables and makes this algorithm suitable for a small dataset. Thus, CART does not need a huge amount of data for training, requires few data preparation and can make accurate decisions based on few data observations which makes it suitable for our work.

In order to create a decision tree, it is important to select the best attribute for tree nodes. For this purpose, CART uses uses Gini Impurity as metric to know to which class an object belongs. Mathematically, it can be represented as:

$$Gini(n) = 1 - \sum_{i} p(C_i|n)^2 \tag{3.7}$$

where $p(C_i|n)$ is the probability of a node n being the category $C_i$. The CART algorithm uses this metric to make the best split of nodes which is the one with maximum Gini index.

## 3.3 Description of the proposed method

The primary challenges of brain MRI segmentation are intensity non-uniformity and noise which motivates researchers to employ and develop fuzzy approaches. FCM is one of the most frequently used algorithm to perform MRI images segmentation and clustering. As a final step in its different proposed variants, each pixel is assigned to the cluster with the highest membership value and it is always expected to obtain good and accurate results. However, there are cases where membership values are too close to each other and the selection of the highest one can lead to obtaining unreasonable results. Therefore, it is mandatory to provide a better membership representation that can separate the two cases of being sure and being uncertain about the decision to be made. Ghasemi. J et al.[69] proposed a solution that consists in employing Dempster-Shafer theory on extracted features by FCM and performing information fusion to defeat uncertainty and get satisfying and robust results. Motivated by this idea, in this study we propose a robust and evidential fuzzy c-means algorithm for MRI brain image segmentation REFCM.

As we previously mentioned, decision making in the case of too close membership values can lead to unreasonable results. Therefore, inspired by the idea of Ghasemi et al., we propose to interpret the output of both FCM and FRFCM employed on the whole image to mass values based on belief theory. Thus, the cases where membership values are too close will be obvious and well represented. The obtained representation will be helpful in the decision-making process since it emphasized uncertain situations. In the next stage, we perform a data fusion between the two obtained mass matrix in order to reduce uncertainty. The output will be a representative mass matrix that clearly indicates whether we are certain about the membership of a pixel to a specific cluster or we still have doubt. Finally, the decision making process will deal with the two cases differently. In the first one where there is no doubt of the pixel's membership, the pixel will directly be assigned to the cluster that it belongs to. In the other case, we trained a decision tree model to make the right classification. The obtained results are promising and robust to noise and intensity non-uniformity. The block diagram of our proposed method REFCM is shown in the figure 3.1.

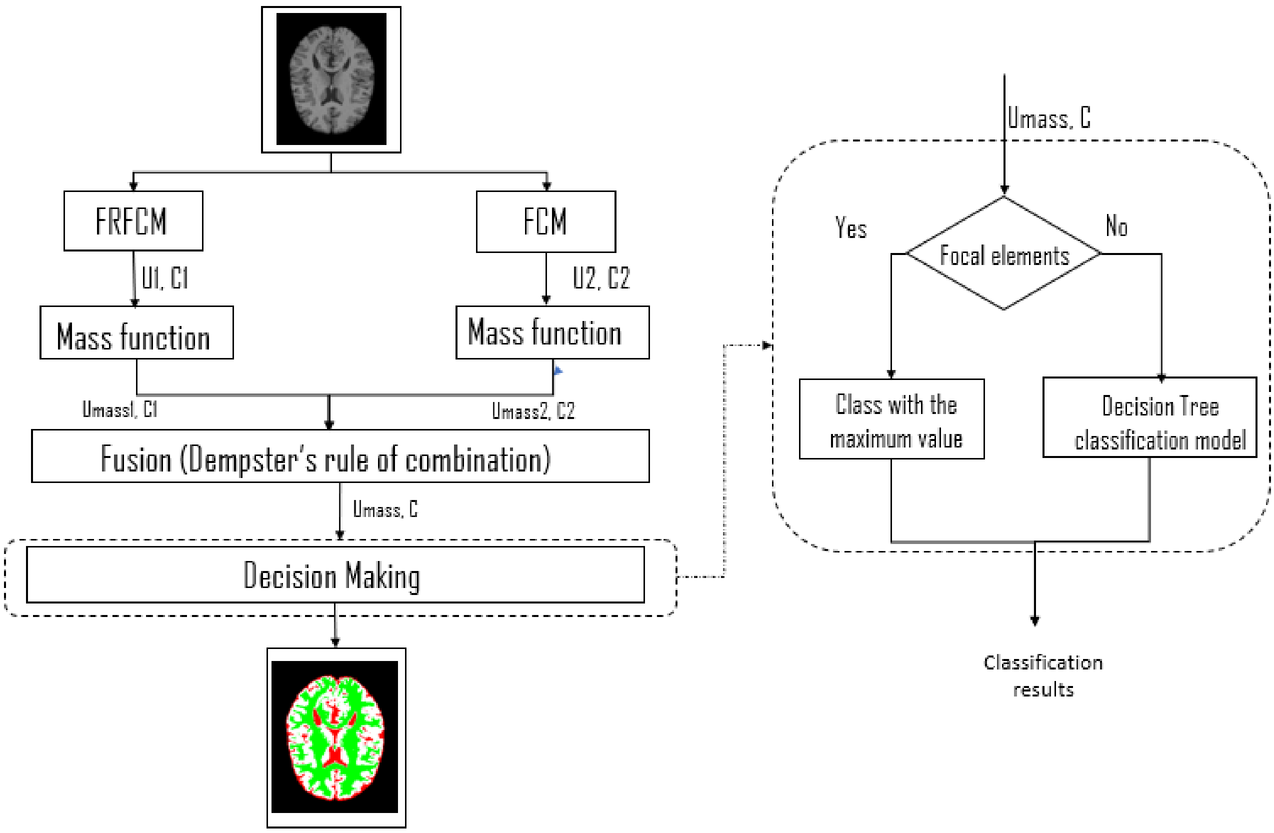


Figure 3.1: Block diagram of REFCM.

We need to dive deeper in details in order to understand each step of our proposed method.

### 3.3.1 FCM and FRFCM

In the first stage, we decided to use both FCM and FRFCM in order to obtain independent information about the same observed image. Thus, we will perform a redundant fusion. This type increases accuracy and reliability as we have explained in the second chapter.

FCM is the classic algorithm that represents the basic method. In fact, it does not involve any filtering or enhancement, it is like going back to the roots. Whereas, FRFCM is the most significant FCM variant that is robust to noise and detail perseverance. It uses morphological reconstruction and median filtering to obtain better results. Besides, it performs its calculation on the image histogram rather than pixels. Their combination can not be but enriching. In fact, even though FRFCM can persevere more details compared to other variants, the filtering process still can affect this perseverance. Therefore, going back to the roots will be beneficial to increase the certainty.

The membership partition matrix obtained from both FRFCM and FCM are respectively named $U_1$ and $U_2$. Similar to the clusters $C_1$ and $C_2$.

### 3.3.2 Belief structure

In the second step, we interpreted the output of both FCM and FRFCM employed on the whole image to mass values based on belief theory., we built a belief structure starting from the output of the two methods.

In our work, we aim to classify the MRI brain images into the three brain tissues: Gray Matter (GM), White Matter (WM) and CerebroSpinal Fluid (CSF). In order to perform a correct clustering, the image background (B) must be taking into consideration as a group that needs to be classified. As a result, our frame of discernment becomes $\Omega = \{B, CSF, GM, WM\}$ and the power set of $\Omega$ is $P(\Omega) = \{\{B\}, \{CSF\}, \{GM\}, \{WM\}, \{B, CSF\}, \{B, GM\}, \{B, WM\}, \{CSF, GM\}, \{CSF, WM\}, \{GM, WM\}, \{B, CSF, GM\}, \{B, CSF, WM\}, \{B, GM, WM\}, \{CSF, GM, WM\}, \Omega, \{\emptyset\}\}$. The process of building a belief structure depends on the membership values (MVs) that are too close and on how much they can express uncertainty.

First of all, we start by computing the ratios between the maximum membership values and the others. Thus, we can identify the MVs that are too close to the one considered as the right indication of the pixel's cluster by FCM and FRFCM. Based on these ratios, four situations will be considered, the case of no uncertainty (NU), semi uncertainty (SU) with one other cluster center, perfect uncertainty (PU) with one other cluster center and both perfect uncertainty and semi uncertainty (PUSU) with two other cluster centers. These situations were defined by the selection of two thresholds $\alpha = 1.5$ and $\beta = 3$ to which we compared the obtained ratios. They control the boundaries between the different situations as show in the figure below.

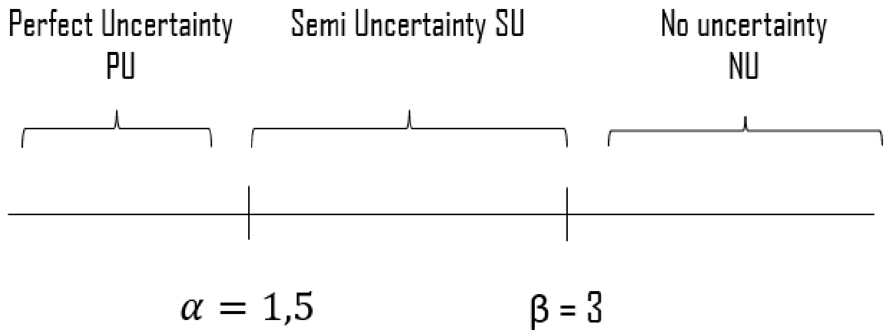


Figure 3.2: Basic three situations and thresholds.

Let U be the membership partition matrix, obtained from the FCM variant, be $U = (\mu_{ij})_{c*n}$ where 'n' is the number of total pixels and c is the number of clusters and let $U_{mass}$ the mass matrix that we are going to build be $U_{mass} = (\delta_{idx\{s\}j})_{2^c*n}$ where $idx\{s\}$ represents the index of the set s in the power set $P(\Omega)$.

#### 3.3.2.1 No Uncertainty

NU is the situation in which the ratio of the maximum membership value with other three values is greater than $\beta$. In this case, the highest MV is too far from the other three and thus we are certain about the membership of the pixel to that specific cluster. Therefore, the MVs are interpreted to mass values with no change. In other words, the same MVs will be assigned to singleton the subsets of $\Omega$. In this situation, the focal element will remain in the subsets $\{B\}, \{CSF\}, \{GM\} and \{WM\}$. $\forall s \in \Omega, \delta_{idx\{s\}j} = \mu_{ij}$ where 'i' is the index of the set s in U.

#### 3.3.2.2 Semi Uncertainty

SU is when one of the ratios is between the two selected threshold and the remaining ratios are higher than $\beta$. It means that a MV of another cluster is considered a little close to the one having the highest value. In order to deal with this uncertainty, we transfer it to the mutual set containing these two clusters. We can express this type of uncertainty based an uncertainty distance defined as:

$$ud_{\{l\}\{q\}} = \frac{\mu_{i_{\{l\}}j} - \mu_{i_{\{q\}}j}}{\beta - \alpha} \tag{3.8}$$

Where:

- $\{l\}$ and $\{q\}$ are the two sets having uncertainty and the MV of $\{l\}$ is higher than the one of $\{q\}$
- $i_{\{l\}}$ is the index of the set $\{l\}$ in U.
- $i_{\{q\}}$ is the index of the set $\{q\}$ in U.

And we need to assign the right value to the mass matrix as follows:

$$\delta_{ind\{l\}j} = \mu_{i_{\{l\}}j} - \frac{ud_{\{l\}\{q\}}}{2}$$

$$\delta_{ind\{q\}j} = \mu_{i_{\{q\}}j} - \frac{ud_{\{l\}\{q\}}}{2}$$

$$\delta_{ind\{\{q\},\{l\}\}j} = \frac{ud_{\{l\}\{q\}}}{2}$$

where $ind\{\{q\},\{l\}\}$ is the index of the set containing both $\{l\}$ and $\{q\}$ subsets.

#### 3.3.2.3 Perfect uncertainty

In the PU situation, one of the ratios is smaller than $\alpha$ and the other ratios are higher than $\beta$. It means that a MV of another cluster is considered too close to the one having the highest value. In other words, they have nearly similar MVs. In this case, we represent uncertainty as follows:

$$\delta_{ind\{l\}j} = \delta_{ind\{q\}j} = \delta_{ind\{\{q\},\{l\}\}j} = \frac{\mu_{i_{\{l\}}j} + \mu_{i_{\{q\}}j}}{3} \tag{3.9}$$

#### 3.3.2.4 Perfect and Semi uncertainties

In the PUSU situation, one of the ratios is smaller than $\alpha$ and another one ratios is between the two selected threshold and the remaining ratios are higher than $\beta$. It means that a MV of another cluster is considered a little close to the one having the highest value and another MV of another cluster is considered too close to the one having the highest value and nearly similar. In this case, we consider the ratio between the two other MVs having uncertainty with the highest MV. Therefore, two sub-categories of situations appear.

In the first one, the new calculated ratio is smaller than $\alpha$ which means that the two clusters having uncertainty with the cluster that have the highest MV, in their turn, they have PU. In this case, we firstly deal with the other two clusters rather than the one having the maximum MV using the PU mass assignment formula:

$$\delta_{ind\{l\}j} = \delta_{ind\{q\}j} = \delta_{ind\{\{q\},\{l\}\}j} = \frac{\mu_{i_{\{l\}}j} + \mu_{i_{\{q\}}j}}{3}$$

Where: $\{l\}$ and $\{q\}$ are the two sets having PU, the MV of $\{l\}$ is higher then the one of $\{q\}$ and $\{l\}$ and $\{q\}$ are both different from the one having the highest MV value.
We also assign the other MV to singleton subsets as follows:
$\forall s \in \Omega, s \neq l$ and $s \neq q, \delta_{idx\{s\}j} = \mu_{ij}$ where 'i' is the index of the set s in U.
In this case, we will deal as if the cluster having the highest MV $\{h\}$ has a SU with $\{q\}$, $\{l\}$ and $\{\{l\},\{q\}\}$. So, we compute the uncertainty distance in this case as follows:

$$ud_{\{h\}\{l\}} = ud_{\{h\}\{q\}} = ud_{\{h\}\{\{l\},\{q\}\}} = \frac{\delta_{ind\{h\}j} - \delta_{ind\{l\}j}}{\beta - \alpha}$$

Then, we represent uncertainty as follows:

$$\delta_{ind\{h\}j} = \delta_{ind\{h\}j} - \frac{ud_{\{h\}\{l\}}}{4}$$

$$\delta_{ind\{l\}j} = \delta_{ind\{q\}j} = \delta_{ind\{\{l\},\{q\}\}j} = \delta_{ind\{l\}j} - \frac{ud_{\{h\}\{l\}}}{4}$$

$$\delta_{ind\{\{h\},\{l\}\}j} = \delta_{ind\{\{h\},\{q\}\}j} = \delta_{ind\{\{h\},\{q\},\{l\}\}j} = \frac{2 * ud_{\{h\}\{l\}}}{4}$$

In the second sub-category, the new calculated ratio is between the two selected threshold which means that the two clusters having uncertainty with the cluster that have the highest MV, in their turn, they have SU. In this case, we deal with the cluster having the maximum MV and the cluster that has a PU with it with same concept and formula. Then, we turn to the SU to get the remaining cluster's mass values.

#### 3.3.2.5 Data fusion

As we previously indicated, the membership partition matrix obtained from both FRFCM and FCM are respectively named $U_1$ and $U_2$. Similar to the clusters $C_1$ and $C_2$.Then, the process of uncertainty representation is achieved by obtaining two mass matrix respectively named $U_{mass_1}$ and $U_{mass_2}$ where $U_{mass_1} = (\delta^{(1)}_{idx\{s\}j})_{2^c*n}$ and $U_{mass_2} = (\delta^{(2)}_{idx\{s\}j})_{2^c*n}$. The clusters $C_1$ and $C_2$ remain the same.

Finally, we perform data fusion on $U_{mass_1}$ and $U_{mass_2}$ using Dempster's rule of combination. Then, the general mass matrix $U_{mass}$will be used for decision making.We also calculate the new general clusters using the average of $C_1$ and $C_2$ to get the general clusters C.

### 3.3.3 Decision Making

The last step of our proposed method is the decision-making. It is performed on the obtained matrix from the fusion process. The main idea is to separate the pixels with uncertainty from those having no doubt about their cluster of membership. In latter group of pixels, the only focal elements are those of MVs to the main four clusters; the background, GM, WM and CSF and all the other MVs are equal to zero. Thus, they are directly assigned to their cluster of membership based on the highest MV. Whereas, the pixels having membership uncertainty will be classified using a decision tree. We used the CART algorithm for this purpose. Firstly, we collected data by running the REFCM's previous steps in order to get the general mass matrix. Then, we associated each pixel with its category from the image's ground truth(GT). After that, we performed data cleaning in order to leave only the uncertain values. Finally, we trained our model to make it able of making predictions.

## 3.4 Experimental results

In this section, we will show effectiveness and robustness of REFCM method by comparing it with other methods used in the field.

### 3.4.1 Dataset

In order to evaluate the quality of our method's results, we use three volumetric (3D) MR images from BrainWeb (simulated images). Gray maatter, white matter and cerebrospinal fluid were the three considered components.

The images dimensions are 181 x 217 x 181 with T1-weighted modality and voxels =1x1x1 mm. We tested four level of noise 0%, 3%, 5% and 9% with different intensilty non-uniformity levels 0%, 20% and 40%.

### 3.4.2 Evaluation metrics

To perform an efficient evaluation, we compared the classified image with its ground truth (GT). We used several evaluation metrics which are **Dice Coefficient**, **accuracy**, **precision**.

Firstly, we need to make the following definitions:

- **True Positive (TP)**: The cases in which the model predicts the positive class correctly.
- **True Negative (TN)**: The cases in which the model predicts the negative class correctly.
- **False Positive (FP)**: The cases in which the model predicts the positive class incorrectly.
- **False Negative (FN)**: The cases in which the model predicts the negative class incorrectly.

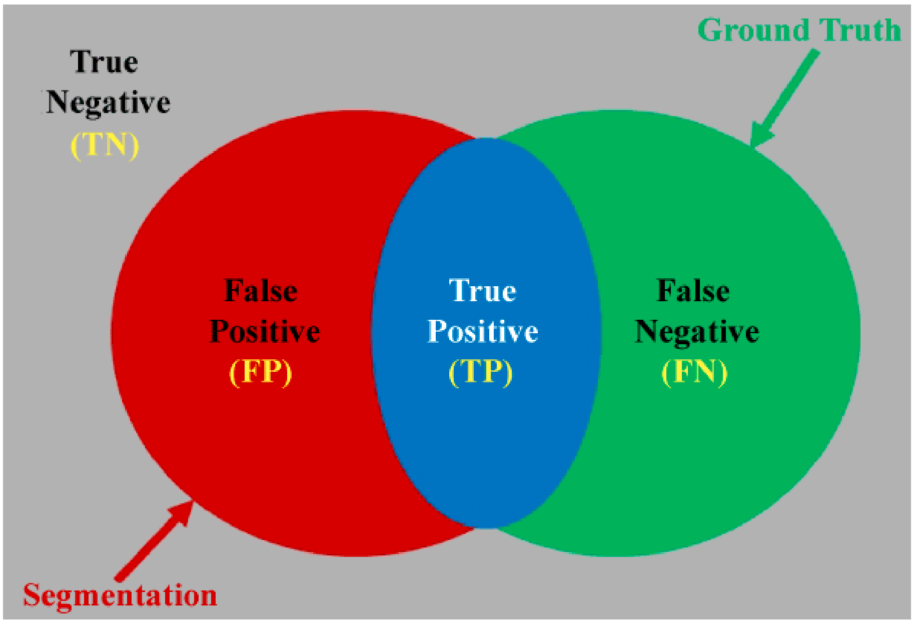


Figure 3.3: TP,FP, FN and TN.

The evaluation metrics that we have used are calculated based on TP, TN, FP and FN [71]:

- **Dice Coefficient (DC)** [72]: It is a metric that measures the similarity between the classified image and its ground truth. Let the classified image be $\hat{A}$ and its ground truth be $A^*$, DC is defined as:

$$DC = \frac{2|\hat{A} \cap A^*|}{|\hat{A} \cup A^*|} = \frac{2TP}{2TP + FP + FN} \tag{3.10}$$

- **Precision** [73]: also called the positive predictive value. It gives us a measure of the relevant data points.Thus, it is used in validation of medical images.

$$Precision = \frac{TP}{TP + FP} \tag{3.11}$$

- **Accuracy** [73]: It measures how often the algorithm classifies a data point correctly. This metric is used when the data set is balanced.

$$Accuracy = \frac{TP + TN}{TP + FP + TN + FN} \tag{3.12}$$

### 3.4.3 Results and discussion

We evaluated our method based on the different evaluation metrics mentioned in the previous section. The table 3.1 presents the different evaluation metrics employed to evaluate our proposed method in different noise and intensity non-uniformity (IN) values.

| Noise(%) IN(%) | Dice Coefficient | Precision | Accuracy |
|---|---|---|---|
| 0 % 0% | 97.3 | 98.1 | 99.1 |
| 0% 4% | 94.2 | 95 | 98.03 |
| 3% 0% | 95.6 | 96.5 | 98.6 |
| 3% 20% | 95.1 | 95.9 | 98.4 |
| 5% 20% | 94.27 | 95.1 | 98.17 |
| 9% 40% | 87.1 | 87.7 | 95.7 |

Table 3.1: Metrics Evaluation of our method.

We used the DC in order to make a meaningful and a fair comparison between our proposed method and some other FCM variants in different noise levels and NI values as show in the table 3.2.

| Noise(%) IN(%) | FCM | FRFCM | REFCM (our method) |
|---|---|---|---|
| 0% 0% | **97.54** | 96.5 | 97.3 |
| 0% 40% | 87.26 | 92.34 | **94.2** |
| 3% 0% | 77.8 | 93.43 | **95.6** |
| 3% 20% | 77.57 | 93.2 | **95.1** |
| 5% 20% | 67.4 | 92.43 | **94.27** |
| 9% 20% | 60.62 | 85.29 | **87.1** |

Table 3.2: Comparison between variant based on DC.

As shows our method exceed the other variants in terms of similarity to the ground truth and the table 3.3 shows the results obtained from our method and from FRFCM in different noise levels and NI values. These segmentation are employed on the slice 95 and 85 of the first 3D MR image from BrainWeb dataset.

| Noise(%) IN(%) | Original | FRFCM | REFCM (our method) |
|---|---|---|---|
| 0% 0% |  |  | 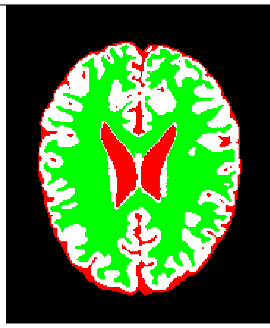 |
| 0% 40% | 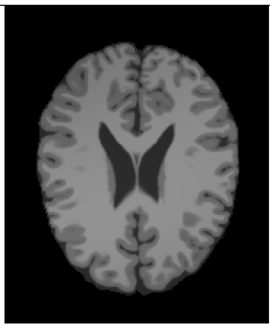 |  | 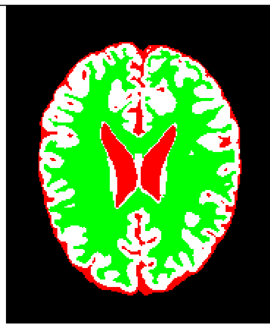 |
| 3% 0% | 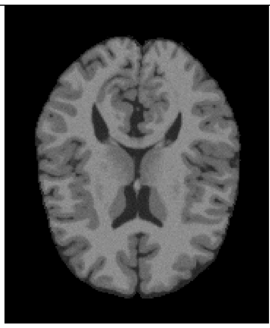 | 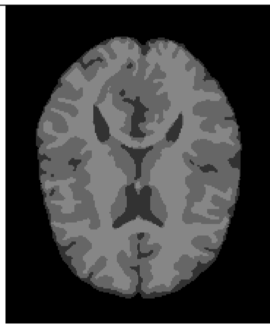 | 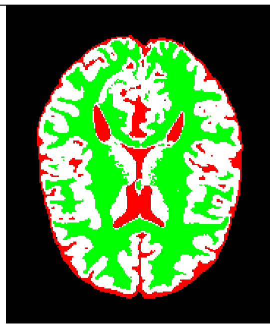 |
| 5% 20% | 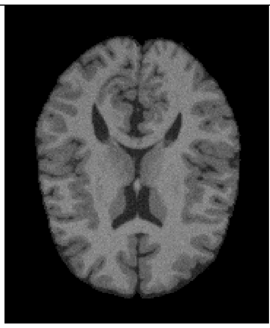 | 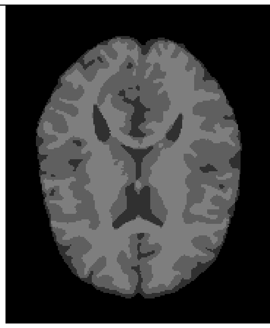 | 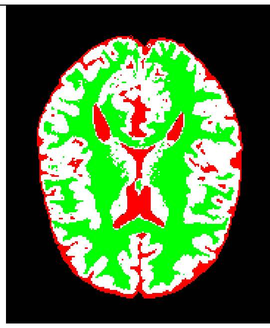 |
| 9% 40% |  | 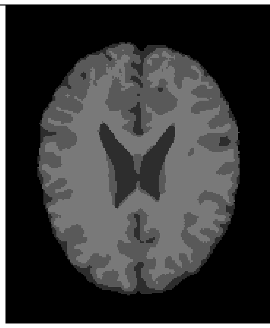 | 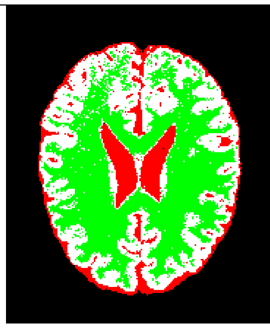 |

Table 3.3: The output from FRFCM and REFCM.

Our method has proven better results and better classification thanks to the new representation uncertainty. From that point, it is important to visualize the different region of an image that can have this doubt. The figure below shows the pixels having membership uncertainty in blue.

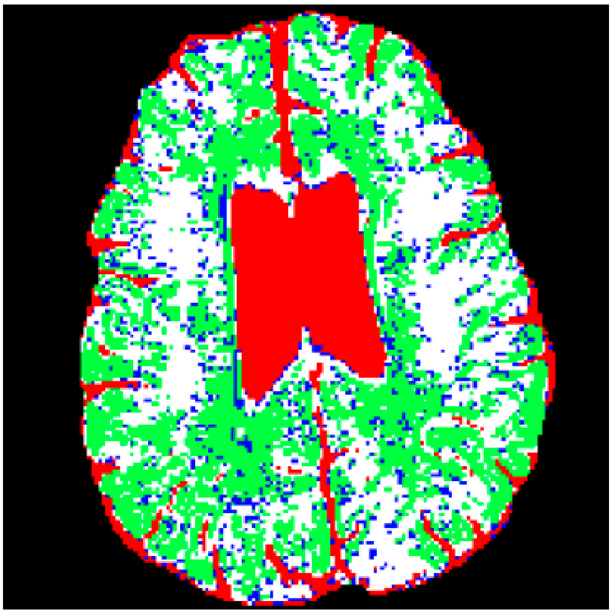

Figure 3.4: Uncertain points.

We can notice that the uncertain points are especially located in the edges and details. In these parts, we can find the intensity changing and overlapping.
The decision tree deals with this uncertainty and the previously shown results are obtained.

## 3.5 Conclusion

In this research work, we have proposed a new Machine Learning method for the segmentation and classification of the three brain tissues from MRI images. In fact, we provided a better representation for uncertainty in the image leading to easier decision making process. In addition, the evaluation of our proposed solution as well as its comparison with other state-of-the-art methods have shown its effectiveness and its robustness. In fact, the quantitative results were better than the other methods.

# Conclusion and Future Work

This dissertation is in the field of medical imaging and more precisely MRI. In fact, the study that we have conducted during this master thesis attempts to develop a new method based on Machine Learning for three brain tissues segmentation and classification in MRI images. Our work was mainly based on image processing and the fundamentals of brain anatomy.

By presenting the general context of our work in the first chapter, we were able to better understand and dive deeper in details related to our research. First of all, we presented the clinical motivation in which we mentioned some diseases that can affect the nervous system and cause neurological disorder. Then, we explained how does the system of medical imaging operates and the main artifacts that can be caused during the image acquisition process. Finally, introduced the challenges of our research work and its objectives.

In the second chapter, we explained the theoretical background and we went through state-of-the-art methods in the field of brain MRI images segmentation. Then, we presented the data fusion approach in both probability and evidential theories.

The third chapter was dedicated to present our contribution. In fact, we proposed a new representation for uncertainty and membership partition from the output of FCM and FR-FCM. Indeed, the combination of the two algorithms was enriching and reduced uncertainty. the new membership partition representation allowed to divide the decision making process into two categories. In the first one, the pixel is directly assigned to its cluster center because its MV is too higher than the others and no uncertainty is associated with these type of pixels. Whereas, for the other category, we trained a decision tree in order to be able to choose the right cluster for pixels having some uncertainty in their membership.

Our proposed method REFCM can be described briefly in three steps:

1. New representation for membership partition based on Dempster-Shafer Theory.
2. Data fusion from the new represented output of FCM and FRFCM.
3. Decision making on separate groups from our data. One group is assigned directly to the right cluster and the other is classified using a decision tree.

After that, our method were tested using three volumetric (3D) MR images from Brain-Web. Then, we performed an evaluation of our work using the dice coefficient and we compared the obtained results with other variants. Our method showed robustness and effectiveness dealing with several artifacts mainly the noise and intensity non-uniformity. In fact, the results obtained for our method in term of accuracy have exceeded the other variants.

Even though the good results proved for our solution, the computational complexity needs to be improved and optimized. In fact, the use of both two FCM variants the fusion operator have increased the computational complexity. As a result, in perspective, we need to work on overcoming the challenge of time cost. In fact, it can be resolved using super-pixel segmentation. In that case, we will be able to fuse more variants together in order to increase certainty and have a more accurate results.

# References

[1] Stephen G. Waxman. "Clinical Neuroanatomy". In: New York: MCGraw Hill, 2003. ISBN: 978-3-030-32380-6.

[2] and Vernice Jackson-Lewis Serge Przedborski Miquel Vila. "Series Introduction: Neurodegeneration: What is it and where are we?" In: *J Clin Invest.* 111(1) (Jan. 2003), pp. 3–10. DOI: `10.1172/JCI17522`.

[3] Alzheimer's association. "Alzheimer's disease facts and figures". In: 2020.

[4] World Health Organization. "Weekly epidemiological update on COVID-19". In: Nov. 2021.

[5] Yuanyuan Qin et al. "Long-term microstructure and cerebral blood flow changes in patients recovered from COVID-19 without neurological manifestations". In: *J Clin Invest* 131(8) (Feb. 2021). DOI: `https://doi.org/10.1172/JCI147329.`.

[6] Shaibu Mohammed Atabo Abubakar Abubakar Umar. "A review of imaging techniques in scientific research/clinical diagnosis". In: *MOJ Anatomy Physiology* 131(8) (Oct. 2019), pp. 175–183.

[7] Isaac Bankman. "Handbook of Medical Image Processing and Analysis". In: Dec. 2008.

[8] Arati S Panchbhai. "Wilhelm Conrad Röntgen and the discovery of X-rays: Revisited after centennial". In: *Journal of Indian Academy of Oral Medicine Radiology* 27(1) (Oct. 2015), pp. 90–95.

[9] William G. Bradley. "History of Medical Imaging". In: *Proceedings of the American Philosophical Society* 152(3) (Sept. 2008), pp. 349–361.

[10] Gilbert Thompson. "Pioneers of Medicine Without a Nobel Prize". In: Apr. 2014, pp. 169–180. DOI: `https://doi.org/10.1142/p922`.

[11] G N Hounsfield. “Computerized transverse axial scanning (tomography). 1. Description of system”. In: *Br J Radiol* 46(552) (Dec. 1973), pp. 1016–22. DOI: 10.1259/0007-1285-46-552-1016.

[12] Vadim Kuperman. “Basic Principles of Nuclear Magnetic Resonance”. In: *Magnetic Resonance Imaging: Physical Principles and Applications*. 2000.

[13] *Magnetic Resonance Imaging (MRI) of the Brain and Spine: Basics*. URL: https://case.edu/med/neurology/NR/MRI%20Basics.html.

[14] *LES EXAMENS Echographies Obstétricale*. URL: https://www.risf.fr/les-examens/echographie/echographies-obstetricale/.

[15] *Les Kystes biliaires (Simple Hepatic Cyst)*. URL: http://www.isurgery.ch/Isurgery/Blog_Isurgery/Entrees/2015/4/11_Les_Kystes_biliaires_(Simple_Hepatic_Cyst).html.

[16] Ashish GAIDHANE. *MRI System Market Size Share | Global Industry Report Till 2025*. URL: https://web.babbler.fr/document/show/mri-system-market-size-share-global-industry-report-till-2025#/.

[17] Vijay P B Grover et al. “Magnetic Resonance Imaging: Principles and Techniques: Lessons for Clinicians”. In: *J Clin Exp Hepatol* 5(3) (Sept. 2015), pp. 246–55. DOI: 10.1016/j.jceh.2015.08.001.

[18] Abir Berger. “How does it work? Magnetic resonance imaging”. In: *BMJ* 324(7328) (Jan. 2002), p. 35.

[19] B. Kastler et al. “Introduction à l’imagerie par résonance magnétique (1) : magnétisme, résonance, excitation et relaxation”. In: *La lettre du Neurologue* 4(4) (Sept. 2000).

[20] *Qu’est ce que l’IRM?* URL: https://www.im2p.fr/examen-qu-est-ce-que-l-irm,21.html.

[21] *Non-Ionizing radiation in MRI*. URL: http://theenergyofradiation.blogspot.com/2016/12/characteristic-of-mri.html.

[22] Gregory M Preboske et al. “Common MRI acquisition non-idealities significantly impact the output of the boundary shift integral method of measuring brain atrophy on serial MRI”. In: *Neuroimage* 30(4) (May 2006), pp. 1196–202.

[23] J L Prince D L Pham C Xu. “Current methods in medical image segmentation”. In: *Annu Rev Biomed Eng* 11 (2000). DOI: 10.1146/annurev.bioeng.2.1.315.

[24] S I Bekkelund C Pierre-Jerome A Arslan. "MRI of the spine and spinal cord: imaging techniques, normal anatomy, artifacts, and pitfalls". In: *J Manipulative Physiol Ther* 23(7) (Sept. 2000).

[25] John G. SledG. Bruce Pike. "Understanding intensity non-uniformity in MRI". In: *International Conference on Medical Image Computing and Computer-Assisted Intervention* (June 2006), pp. 614–622. DOI: 10.5614/itbj.ict.res.appl.2017.11.3.3.

[26] G B Pike J G Sled. "Standing-wave and RF penetration artifacts caused by elliptic geometry: an electrodynamic analysis of MRI". In: *IEEE Trans Med Imaging* 17(4) (Aug. 1998), pp. 653–62.

[27] A Simmons et al. "Sources of intensity nonuniformity in spin echo images at 1.5 T". In: *Magn Reson Med* 32(1) (July 1994).

[28] Karol Miller. "Introduction to Brain Anatomy". In: *Biomechanics of the Brain*. 2011.

[29] *Architecture du cerveau*. URL: https://parlonssciences.ca/ressources-pedagogiques/documents-dinformation/architecture-du-cerveau.

[30] URL: https://www.chegg.com/flashcards/chapter-7-2-nervous-control-d1bc1149-f88c-4c25-a50c-b61f05227f6e/deck.

[31] Thomas Schneider-Axmann et al. "Relation between cerebrospinal fluid, gray matter and white matter changes in families with schizophrenia". In: *J Psychiatr Res* 40(7) (Oct. 2006), pp. 646–55.

[32] Roya Babaie Aghdam et al. "Challenges in Brain Magnetic Resonance Image Segmentation". In: *American Scientific Research Journal for Engineering, Technology and Sciences* 27(1) (2017), pp. 122–138.

[33] Hesham F. Ali Wedad S. Salem Ahmed F. Seddik. "A Review on Brain MRI Image Segmentation". In: (2013).

[34] PunamThakare. "A Study of Image Segmentation and Edge Detection Techniques". In: *International Journal on Computer Science and Engineering* 3(2) (2011), pp. 259–267.

[35] Jitendra Malik Pablo Arbeláez M. Maire. "From contours to regions: An empirical evaluation". In: *IEEE Conference on Computer Vision and Pattern Recognition* (June 2009).

[36] K. Jeevitha A. Iyswariya V. RamKumar S. Mahaboob Basha V. Praveen Kumar. "A REVIEW ON VARIOUS SEGMENTATION TECHNIQUES IN IMAGE PROCESSS-ING". In: *European Journal of Molecular  Clinical Medicine* 7(4) (2020), pp. 1342–1348.

[37] Mihaela Ionescu et al. "Comparative study of contour detection methods for intestinal sessile polyps". In: *E-Health and Bioengineering Conference (EHB)* (Jan. 2013).

[38] Himanshu Aggarwal. "Study and Comparison of Various Image Edge Detection Techniques". In: 3(1) (Mar. 2009).

[39] Michele Peporte; Dana E. Ilea; Eilish Twomey; Paul F. Whelan. "A Morphological Approach for Infant Brain Segmentation in MRI Data". In: *Irish Machine Vision and Image Processing Conference* (2011).

[40] I.Ali. "DIGITAL IMAGES EDGE DETECTION USING MATHEMATICAL MORPHOLOGY OPERATIONS Hanna". In: (2013).

[41] Pratibha Goyal Manjot Kaur. "A Review on Region Based Segmentation". In: *International Journal of Science and Research (IJSR)* 4(4) (Apr. 2015).

[42] Devanand Padha Aarish Shafi Dar. "Medical Image Segmentation A Review of Recent Techniques, Advancements and a Comprehensive Comparison". In: *International Journal of Computer Sciences and Engineering* 7(7) (July 2019), pp. 114–124.

[43] PElsa D. Angelini et al. "Brain MRI Segmentation with Multiphase Minimal Partitioning: A Comparative Study". In: *International Journal of Biomedical Imaging* 2007 (Apr. 2007), pp. 1–15.

[44] Grossberg Hu and Mageras. "Survey of Recent Volumetric Medical Image Segmentation Techniques". In: *Biomedical Engineering*. 2009. URL: `http://www.intechopen.com/books/biomedical-engineering/survey-of-recent-volumetric-medical-imagesegmentation-%20techniques`.

[45] Bart Goossens Ivana Despotović and Wilfried Philips. "MRI Segmentation of the Human Brain: Challenges, Methods, and Applications". In: *Comput Math Methods Med* (Mar. 2015).

[46] P. Hiremath D. Shubhangi. "Support vector machine (SVM) classifier for brain tumor detection". In: *Proceedings of the International Conference on Advances in Computing, Communication and Control* (Jan. 2009).

[47] Celina Imielinska et al. "Hybrid Segmentation Methods". In: *Insight into Images*. 2004.

[48] S. Kirillova A. Zotin K. Simonov. "Edge detection in MRI brain tumor images based on fuzzy C-means clustering". In: *Procedia Computer Science* 126 (2018), pp. 1261–1270.

[49] Songfeng Lu Ismail Yaqub Maolood Yahya Eneid Abdulridha Al-Salhi. "Thresholding for Medical Image Segmentation for Cancer using Fuzzy Entropy with Level Set Algorithm". In: *Open Med (Wars).* 13 (Sept. 2018), pp. 374–383. DOI: 10.1515/med-2018-0056.

[50] N. Prakash Janardhan Chidadala Sri Nagesh Maganty. "Automatic Seeded Selection Region Growing Algorithm for Effective MRI Brain Image Segmentation and Classification". In: *International Conference on Intelligent Computing and Communication Technologies* (Dec. 2020), pp. 836–844. DOI: https://doi.org/10.1007/978-981-13-8461-5_95.

[51] M. T. Manzuri Shalmani Ali Ahmadvand Sahar Yousefi. "A novel Markov random field model based on region adjacency graph for T1 magnetic resonance imaging brain segmentation". In: *International Journal of Imaging Systems and Technology* 27(1) (Mar. 2017), pp. 78–88. DOI: https://doi.org/10.1002/ima.22212.

[52] Mahmoud Neji Ahmed Kharrat. "A System for Brain Image Segmentation and Classification Based on Three-Dimensional Convolutional Neural Network". In: *Computación y Sistemas* 24(4) (2020), pp. 1617–1626.

[53] Wiharto Wiharto and Esti Suryani. "The Comparison of Clustering Algorithms K-Means and Fuzzy C-Means for Segmentation Retinal Blood Vessels". In: *Acta Inform Med* 28(1) (Mar. 2020), pp. 42–47. DOI: 10.5455/aim.2020.28.42-47.

[54] WilliamFull James C.Bezdek RobertEhrlich. "FCM: The fuzzy c-means clustering algorithm". In: *Computers Geosciences* 10 (Dec. 1984), pp. 191–203. DOI: https://doi.org/10.1016/0098-3004(84)90020-7.

[55] M.N. Ahmed; S.M. Yamany; N. Mohamed; A.A. Farag; T. Moriarty. "A modified fuzzy c-means algorithm for bias field estimation and segmentation of MRI data". In: *IEEE Trans. Med. Imag.* 21(3) (Mar. 2002), pp. 193–199.

[56] S. Chen and D. Zhang. "Robust image segmentation using FCM with spatial constraints based on new kernel-induced distance measure". In: *IEEE Trans. Syst.* 34(4) (Aug. 2004), pp. 1907–1916. DOI: 10.5614/itbj.ict.res.appl.2017.11.3.3.

[57] L. Szilagyi et al. “MR brain image segmentation using an enhanced fuzzy c-means algorithm”. In: *Proc. 25th Annu. Int. Conf. IEEE EMBS* 11 (2003), pp. 17–21.

[58] S. Chen W. Cai and D. Zhang. “Fast and robust fuzzy c-means clustering algorithms incorporating local information for image segmentation”. In: *Pattern Recognit.* 11 (Mar. 2007), pp. 825–838.

[59] S. Krinidis and V. Chatzis. “A robust fuzzy local information c-means clustering algorithm”. In: *IEEE Trans. Image Process.* 19 (Mar. 2010), pp. 1328–1337.

[60] S. Shi M. Gong Y. Liang and J. Ma. “Fuzzy c-means clustering with local information and kernel metric for image segmentation”. In: *IEEE Trans. Image Process.,* 22 (Feb. 2013), pp. 573–584.

[61] L. Cheng Z. Zhao and G. Cheng. “Neighbourhood weighted fuzzy cmeans clustering algorithm for image segmentation”. In: *IET Image Process.* 8 (Mar. 2014), pp. 150–161.

[62] et al. Tao Lei. “Significantly Fast and Robust Fuzzy C-Means Clustering Algorithm Based on Morphological Reconstruction and Membership Filtering”. In: *IEEE TRANSACTIONS ON FUZZY SYSTEMS* 26(5) (2017).

[63] Federico Castanedo. “A Review of Data Fusion Techniques”. In: *Scientific World Journal* (Aug. 2013).

[64] Jean-Louis Féménias. “Probabilités et statistique pour les sciences physiques”. In: Mar. 2003. ISBN: 978-2-10-005972-0978-3-030-32380-6.

[65] Sebtel Press. “Bayes’ Rule: A Tutorial Introduction to Bayesian Analysis”. In: June 2013. DOI: `10.13140/2.1.1371.6801`.

[66] Jürg Kohlas Paul-André Monney. “Theory of evidence — A survey of its mathematical foundations, applications and computational aspects”. In: *Zeitschrift für Operations Research* 39 (1994), pp. 35–68.

[67] Subhash Challa Don Koks. “An Introduction to Bayesian and Dempster-Shafer Data Fusion”. In: *DSTO–TR–1436* (2005).

[68] Glenn Shafer. “Dempster’s rule of combination”. In: *International Journal of Approximate Reasoning* 79 (Dec. 2016), pp. 26–40. DOI: `10.5614/itbj.ict.res.appl.2017.11.3.3`.

[69] Jamal Ghasemi et al. "Brain Tissue Segmentation by FCM and Dempster-Shafer Theory". In: *IEE 2011 7th Iranian Conference on Machine Vision and Image Processing* (2011).

[70] S. Jafari S.M. Fakhrahmad L. Zarban. "Uncertain decision tree inductive inference". In: *International Journal of Electronics* (2011).

[71] Abdel Aziz Taha Allan Hanbury. "Metrics for evaluating 3D medical image segmentation: analysis, selection, and tool". In: *BMC Medical Imaging* (Aug. 2015).

[72] Lee R. Dice. "Measures of the Amount of Ecologic Association Between Species". In: *Ecology* 26.3 (1945), pp. 297–302. DOI: https://doi.org/10.2307/1932409. eprint: https://esajournals.onlinelibrary.wiley.com/doi/pdf/10.2307/1932409. URL: https://esajournals.onlinelibrary.wiley.com/doi/abs/10.2307/1932409.

[73] Jayaram K. Udupa, Vicki R. LeBlanc, Ying Zhuge, Celina Imielinska, Hilary Schmidt, Leanne M. Currie, Bruce E. Hirsch, and James Woodburn. "A framework for evaluating image segmentation algorithms". In: *Computerized Medical Imaging and Graphics* 30.2 (2006), pp. 75–87. ISSN: 0895-6111. DOI: https://doi.org/10.1016/j.compmedimag.2005.12.001. URL: https://www.sciencedirect.com/science/article/pii/S089561110500114X.

# *Abstract*

This master thesis was conducted within the context of intelligent image processing and automatic segmentation. In this work, we focused mainly on the classification and the segmentation of three brain tissues from MRI images using Machine Learning. Our contribution consists in improving the partition membership representation with Demspter-Shafer theory and dealing with uncertainty in order to perform classification using a decision tree. We used three volumetric (3D) MR images from BrainWeb as a testing dataset.

**Key words:** MRI, Image segmentation, Classification, Brain tissues, Fuzzy C-means, Dempster-Shafer theory.

---

# *Résumé*

Ce mémoire a été réalisé dans le cadre général du traitement intelligent des images et de la segmentation automatique. Le thème principal de ce travail est la classification et la segmentation des trois tissus du cerveau à partir des images IRM en utilisant une méthode de Machine Learning. Notre contribution consiste à améliorer de la représentation de l'appartenance à une classe en mettant l'accent sur l'incertitude en utilisant la théorie de l'évidence et traiter cette incertitude pour faire une classification précise en utilisant l'arbre de décision. Les données de tests considérées sont les images IRM de la base BrainWeb.

**Mots clés:** Segmentation d'images, Classification, Tissus du cerveau, Fuzzy C-means, Théorie de l'évidence.